DESIGN OF POLY (ALKYLENE OXIDE) GRAFT COPOLYMER CHEMISTRIES FOR IMPROVED ANTISENSE DRUG DELIVERY

by

LAVANYA Y. PEDDADA

A Dissertation submitted to the

Graduate School-New Brunswick

Rutgers, The State University of New Jersey

and

The Graduate School of Biomedical Sciences

University of Medicine and Dentistry of New Jersey

in partial fulfillment of the requirements

for the degree of

Doctor of Philosophy

Graduate Program in Biomedical Engineering

written under the direction of

Charles M. Roth, Ph.D.

and approved by

_____

_____

_____

_____

New Brunswick, New Jersey

January, 2012

ABSTRACT OF THE DISSERTATION

Design of poly (alkylene oxide) graft copolymer chemistries for improved antisense drug delivery

By LAVANYA Y. PEDDADA

Dissertation Director:
Charles M. Roth, Ph.D.

Gene-based therapies hold tremendous promise to treat conditions such as cancer, muscular dystrophy, and cardiovascular disease. Non-viral carriers consisting of synthetic and natural cationic polymers, liposomes, and non-ionic copolymer micelles have demonstrated moderate success in overcoming some of the delivery challenges. At the systemic level, the issues of drug degradation in the bloodstream and poor pharmacological distribution to target disease site exist. At the cellular level, the key barrier involves escape of the carrier and therapeutic cargo from the degradative endolysosomal pathway. Efforts have been made to understand and to design carrier chemistries based on physical properties including particle size, particle surface charge, degree of carrier hydrophilicity/hydrophobicity, polymer conformation, etc. To date, clear design rules based on physicochemical properties have not emerged.

Previously, our group has formulated a multi-component liposome-based carrier system that efficiently delivers antisense oligonucleotide in the absence of serum, but which is considerably less active in the presence of serum. This motivated us to improve the existing carrier chemistry for improved delivery in the presence of extracellular nucleases and serum proteins, while maintaining the function of evading intracellular

barriers. In this dissertation, we provide a comprehensive evaluation of graft copolymers consisting of poly (propylacrylic acid) and poly (alkylene oxide) chemistries with varying degrees of hydrophobicity to hydrophilicity, and describe the influence of this parameter on liposome-mediated antisense gene delivery. First, various steps involved in the antisense gene delivery process including serum-stability, membrane penetration, and endosome membrane lysis was evaluated in vitro. Secondly, we address the hypothesis that liposomes stabilized with poly (alkylene oxide) graft copolymers can improve biodistribution by using a tumor xenograft model that allows us to relate biodistribution profiles to nanoparticle size, surface charge, and polymer architecture. Our findings indicate that the balance of polymer hydrophobicity to hydrophilicity plays a key role in dictating serum-stability and cellular entry in vitro, as well as fate of antisense in vivo.

ACKNOWLEDGEMENT

There are a number of people I would like to thank for all their help and support through my graduate studies. First and foremost, I would like to thank my advisor, Dr. Charles Roth, for his guidance and support through the Ph.D. process. He has been patient and extremely supportive. More importantly, he has given me the independence to pursue my interests and research direction, and this has helped me to grow as a scientist. Next, I would like to thank my committee members: Dr. Devore, Dr. Minko, Dr. Moghe and Dr. Cai. Their scientific input and guidance has been of great value and contributed to the completion of my thesis work.

I would like to acknowledge my funding sources, New Jersey Commission on Cancer Research (NJCCR), Integrative Graduate Education and Research Traineeship (IGERT) and the NIH Grant (2R01EB008278-07), for allowing me to focus all my energies on research, thus helping the project to mature. With these fellowship and funding opportunities I was able to present my work at various conferences, obtain valuable feedback, gain scientific exposure and network with other scientific professionals in the field.

I would like to give credit to the post-docs and senior graduate students who have provided scientific input and mentorship- Dr. Harris, Dr. Joy, Dr. Costache, Dr. Sundaram, Dr. Garbuzenko, Dr. Lee, Dr. Wininger and Dr. Misra. They have provided technical expertise in the areas of polymer synthesis, antisense carrier chemistry, drug delivery, and pharmacokinetics, all of which have been essential is helping this project evolve. As far as support from peers in the chemical and biomedical engineering programs, I would like to specially acknowledge Nuria, Carolyn, Jocie, Elina, Dominik,

Jeffery, Aina and Ankita. I have enjoyed the scientific discussions we've had and leaned on them for moral support. All of these people have become my closest friends during the graduate school experience, making all the years of hardship enjoyable. They have really supported and advised me on many grounds from experimental troubleshooting, project direction, to everyday life. I have learnt a lot from them and wish them success in their scientific endeavors.

Finally, I would like to thank my family for giving me the encouragement and motivation to work through the tough times in graduate school. My parents have been pillars of support. They have worked hard to provide me with the best education and have helped me stay positive and focused over these years. I cannot thank them enough and I dedicate my achievements to them. I would also like to thank my brother, Chetan, for keeping me in good spirits when things wouldn't work at lab. My in-laws, the Thakers, have also been extremely supportive and curious about science and the work I do, thereby providing me encouragement. My husband, Parth, has been there for me since the time I applied to graduate school and has been a constant source of motivation. He has patiently listened to my problems, provided advice, and even spent many days with me at lab. I could not have completed the Ph.D. without him by my side.

PRIOR PUBLICATIONS

Several sections of this dissertation have been published in journal articles, or are pending external publication. The following publications are acknowledged:

- Certain sections of Chapter 1, the introduction, have been submitted to Accounts of Chemical Research for publication as a perspective article titled, “Poly(alkylene oxide) Copolymers for Nucleic Acid Delivery”. Spring 2012
- Chapter 2 has been published in its entirety and has the following citation: Peddada LY, Harris NK, Devore DI, Roth CM. Novel graft copolymers enhance in vitro delivery of antisense oligonucleotides in the presence of serum. *J Control Release*. 2009 Dec 3; 140(2):134-40.

TABLE OF CONTENTS

LIST OF TABLES

LIST OF FIGURES

LIST OF SCHEMES

KEY ABBREVIATIONS:

ODN: oligonucleotide

DOTAP: N-[1-(2,3-Dioleoyloxy)propyl]-N,N,N-trimethylammonium methyl-sulfate

PPAA: poly (propyl acrylic acid) (referred to as ‘P’ in figures)

DOTAP/ODN: Complexes of DOTAP and ODN formed by electrostatic interactions

PEO/EO: poly (ethylene oxide)/ethylene oxide

PPO/PO: poly (propylene oxide)/propylene oxide

PAO: poly (alkylene oxide), for our purposes this family encompasses poly (ethylene oxide) and Jeffamine family (EO and PO)

‘J70’ or Jeffamine M 2070: Jeffamine M 2070, Molecular weight 2kDa, EO/PO = 3/1 from Huntsman

‘J05’ or Jeffamine M 2005: Jeffamine M 2005, Molecular weight 2kDa, EO/PO = 1/6 from Huntsman

HF: Hydrophilic Factor

RES: Reticuloendothelial system

EPR: Enhanced Permeation Retention

MPS: mononuclear phagocytic system

PDMAEMA: poly(2-dimethylamino)ethylmethacrylate

PEI: polyethyleneimine

CHO: Chinese Hamster Ovary cell line

IP: intraperitoneal

IV: intravenous

CHAPTER 1: INTRODUCTION

1.1 Combination Therapy (antisense and chemotherapy)

The main forms of cancer therapy include surgery, radiation and chemotherapy. The choice of therapy is dependent on factors such as the grade and type of cancer. Chemotherapy is a widely employed treatment modality that is used either prior to or post-surgery, and can be accompanied by radiation, or utilized by itself. The mechanism by which chemotherapeutic agents induce tumor cell death involves the disruption of processes such as mitosis or DNA replication, which prevent tumor cells from multiplying [1, 2]. However, in response, cancer cells develop oncogenic mutations to repair DNA and evade commitment to apoptosis. One of the strategies to improve the effectiveness of chemotherapy involves silencing oncogenes through the mechanism of antisense. Antisense therapy involves using molecules that degrade the mRNA (such as antisense oligonucleotides and siRNAs), which prevent the expression of the target gene, and following this, the synthesis of the protein [3-5]. The use of antisense is particularly attractive for gene targets that are insensitive to inhibition by the use of antibodies or small molecules.

Vitravene, an antisense drug developed by ISIS Pharmaceuticals, has been approved by the FDA as a treatment for patients with AIDS-related retinitis. In the area of oncology, many antisense targets have demonstrated progress in early-phase clinical trials, with Genasense and Affinitak being the two most well-known drugs. Affinitak™ is an antisense agent targeted against PKC-alpha, a protein over-expressed in cancer cells. This protein has been associated with the promotion of growth, development and survival of malignant cells, and resistance to chemotherapy. Genasense is an antisense agent

targeted to Bcl-2, an anti-apoptotic protein that is over-expressed in multiple tumor states such as breast, epithelium, ovarian, and pancreatic [6]. Genasense (G3139) is being actively studied for clinical use in conjunction with several chemotherapy agents, radiation therapy and immunotherapy. Genasense® is being evaluated for its use in combination with agents such as Gleevec®, Rituxan®, paclitaxel, cyclophosphamide, etc, and is currently undergoing clinical trials for treatment of solid tumor [7, 8]. Research groups have demonstrated a synergistic cytotoxic effect by the use of Bcl-2 siRNA in combination with drugs such as paclitaxel, doxorubicin and etoposide [9]. Currently a phase I/II study of Genasense® in combination with doxorubicin and docetaxel is being conducted [10]. Such progress demonstrates the potential of combined treatments of antisense and chemotherapeutic drugs for tumor therapy.

Tumor cells demonstrate defects in processes such as proliferation and apoptosis, as well as the development of drug resistance [11]. The genes involved in the anti-apoptotic pathway represent attractive targets for two reasons: 1) defects in this pathway occur during tumorigenesis, and 2) impairments in this pathway occur as a result of repeated chemotherapy exposure to tumor cells. Although early treatments with chemotherapeutic drugs prove to be effective, repeated exposure of these drugs causes an over-expression of genes that are associated with anti-apoptosis and multi-drug resistance. Effective treatment of human malignancies is hindered due to the development of multidrug resistance to chemotherapy. For example, in breast carcinomas, it has been established that members of the ATP binding cassette (ABC) transporter family that encode efflux pumps are upregulated as a response to the use of chemotherapy. Some of these proteins involved in the drug resistance pathway include multidrug resistance (MDR), multidrug

resistant protein (MRP), and breast cancer resistance protein (BCRP) [12-14]. These genes represent a range of therapeutic targets and hence potential for antisense gene therapy.

1.2. Challenges to nucleic acid delivery

1.2.1 Key systemic challenges (RES and EPR effect)

Carriers are designed to enable successful delivery of therapeutic cargo from the point of injection to the target site of action. At the systemic level, the function of the carrier involves increasing the circulation time of the therapeutic molecule so that it can reach the target tumor site before interaction with blood proteins and degradation by serum nucleases. The undesired organs for accumulation of a nucleic acid or nanoparticle include the liver, kidney, spleen, and lung (unless target disease organs). Accumulation in these organs is dependent on the chemistry of the nucleic acid backbone or nucleic acid conjugate, and in the case of the nanoparticle, its physical properties such as size, degree of protective groups, charge, etc. After IV injection of antisense oligonucleotides, ~80% are detected in the kidney and liver organs [15]. Uncomplexed nucleic acid is rapidly filtered by the glomeruli (40kDa ~ MW cutoff for filtration), while nanoparticles help to prevent this clearance method. A key barrier preventing the uptake of nanoparticles by the tumor is degradation of particles by the mononuclear phagocytic system (MPS), which includes the liver, spleen and bone marrow. First, we discuss the process of opsonization, followed by clearance of foreign material present in the body by phagocytes of the MPS organs. Opsonization in the process by which opsonin proteins in the blood come in contact with a foreign particle, and adsorb onto the particle. Opsonins encompass blood serum proteins such as laminin, fibronectin, C-reactive proteins and

others, as well immunoglobulins and components of the complement system such as C3, C4 and C5 [16, 17]. The opsonins in the bloodstream come in contact with nanoparticles and if unprotected, will bind to these particles and signal the process of phagocytosis. The process of opsonin binding with nanoparticle includes several attractive forces including van der Walls, electrostatic, ionic, hydrophilic/hydrophobic, and others. After the process of opsonization, phagocytosis takes place as a result of recognition of opsonin protein bound to the surface of the nanoparticle. Macrophages, which are typically Kupffer cells, or macrophages of the liver do not directly identify foreign particles, but instead recognize the specific opsonin proteins that mark particles as foreign, thereby initiating the process of destruction [16]. This process is the main clearance mechanism for particles larger than ~10 nm, the cutoff for renal clearance. Although nanoparticles can be modified to increase blood circulation, a majority of the injection dose is lost to MPS uptake, typically leaving 2-10% distributed to the target tissue [18]. The process of phagocytic recognition and clearance from the bloodstream is an important issue to tackle; therefore efforts in the field of nanoparticle delivery have focused on trying to avoid this degradative process. It has been shown that hydrophobic particles are opsonized more rapidly due to the enhanced adsorption of blood serum proteins on these surfaces, compared to hydrophilic particles [19]. This has introduced the field of stealth drug delivery, which has been to coat nanoparticles with hydrophilic moieties that prevent opsonin recognition of the particle, increase blood circulation time, and finally delivery to the target tissues [20, 21]. Figure 1.1 depicts the journey of the antisense drug from the bloodstream to the various organs.

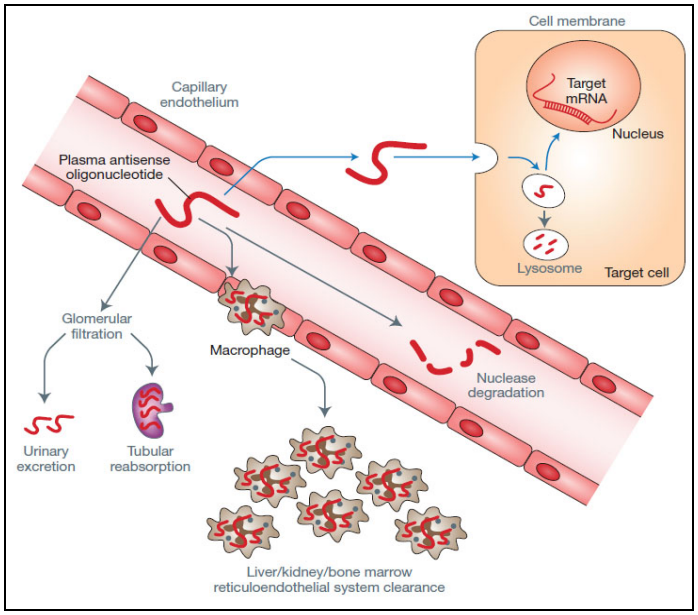

Figure 1.1: Antisense fate following injection [22]

The biology of the tumor plays a role in passive targeting of nanoparticles. Tumor tissues have a characteristic leaky vasculature with large pores and poor lymphatic drainage, which allows for enhanced permeation and retention (EPR) of large particles [23]. The EPR effect can be used to increase uptake and retention of larger-sized particles by allowing preferential accumulation and diffusion into solid tumor tissues, therefore providing a means of passive targeting [24]. The increased permeability of blood vessels in tumors is a result of angiogenesis. Tumors are also marked by a dysfunctional lymphatic drainage system, which allows carriers to be retained at the diseased site and release drug in the proximity of tumor cells. Some studies have shown that the threshold particle size for tumor extravasation is ~ 400nm [25], while other studies have shown that sizes less than 200 nm are favorable for this process [24, 26, 27]. Although passive targeting takes place in solid tumor systems and for those particles that qualify for the

EPR effect, this process is not controlled and can still lead to undesired toxic effects. Furthermore, the leakiness of tumor vasculature is dependent on type of tumor and this is difficult to quantify [28]. Hence, active targeting of tumor cells is a more desired approach to ensuring that nanoparticles bind to specific cells by recognition of specific receptors on the cell surface.

1.2.2 Key intracellular barriers

At the intracellular level, several barriers to antisense delivery exist (Fig. 1.2). These include nanoparticle association with the cell membrane, escape of nanoparticles from endolysosomal degradation, and finally unpackaging of the carrier and antisense to release the antisense to the final destination, that is the cytoplasm of the cell [29]. Several modes of cellular entry including clathrin-mediated endocytosis, caveolae-mediated endocytosis, and membrane fusion have been explored [30]. It has been established that a major barrier to the intracellular delivery of antisense oligonucleotides is their sequestration in endosomes, which eventually fuse with lysosomes, thereby leading to degradation of endosome contents. Methods to traffic this intracellular barrier have exploited the characteristic acidic pH microenvironment of the endosome by utilizing polymers with protonable amines showing buffering capabilities that enable osmotic swelling of the endosome, which results in the burst and release of contents. Other means of achieving release of endosome contents include the use of endosome release peptides (viral or synthetic) with fusogenic capabilities, alkylated carboxylic acids that increase interactions with endosome membrane due to conformational changes in the polymer, or the use of agents such as chloroquine, a weak base [31]. In the field of plasmid DNA delivery, it is known that polyethyleneimine (PEI) is the most efficient

non-viral vector because of its proton-sponge effect, which follows a series of events that involve an influx of protons, osmotic swelling and burst of the endosome, and finally release of the endosome contents [32, 33]. Another popular candidate, poly [2-(dimethylamino) ethyl methacrylate] or pDMAEMA, is partially protonated at physiological pH and completely protonated at acidic pH, thereby causing release of the endosome contents [34]. The properties of polymers have been exploited in order to aid in carrier release from endosomes, thereby successfully delivering therapeutic cargo in its active form.

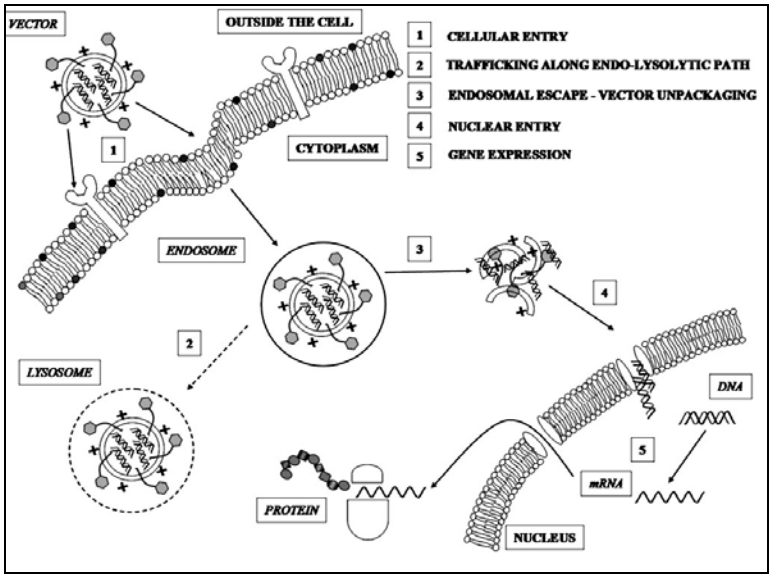

Figure 1.2: Intracellular delivery barriers to ODN delivery [29]

1.3 Carriers for antisense/nucleic acid delivery (polycations and liposomes)

1.3.1. Liposomes

Cationic lipids have been widely employed for the delivery of short interfering RNA (siRNA), antisense oligonucleotides (AONs), and plasmid DNA in several in vitro

and in vivo transfection studies over the past decade [35-37]. In addition to nucleic acid delivery, liposomes have been extensively studied for their ability to deliver chemotherapeutic agents such as doxorubicin and paclitaxel. One of the proposed mechanisms of lipid-mediated intracellular delivery involves the association of the lipid portion of the carrier with the cell membrane to initiate uptake by endocytosis, followed by entrapment of the liposomes in the endosome compartment, leading to fusion of the lipid with the endosome membrane, and finally the release of the cargo into the cytoplasm. The last step is triggered by a flip-flop mechanism.

The constituents of lipids have been varied to achieve desirable characteristics such as membrane penetration. Furthermore, the chemistry of liposomes has been modified to include hydrophilic polymers such as poly (ethylene glycol), PEG, to increase the half-life of the therapeutic cargo, and by the addition of other entities such as targeting ligands and antibodies to achieve targeting [38-41]. The delivery of plasmid DNA using conventional complexes without PEG entities resulted in the detection of plasmid DNA in mice for a period of 12 hrs, while plasmid DNA in PEG-grafted and PEG-added transfection complexes resulted in the detection of DNA for longer periods of time like 24 and 48 hrs, respectively [42]. This is an example demonstrating the importance of modifying liposomes to include features that help to overcome delivery barriers. In this work, the chemistry of the liposome-based carrier is modified to improve the *in vivo* half-life of chemotherapeutic drugs and antisense molecules. Liposomes have also been modified for their drug loading capability. Some clinically approved liposomes systems include Doxil®, a formulation of PEGylated liposome loaded with doxorubicin, and DaunoXome®, liposomal daunorubicin.

1.3.2. pH-sensitive polymers

The use of polycationic carriers such as PLL, PEI and dendrimers has been extensively studied for the delivery of antisense/siRNA molecules. PEI has demonstrated success as a result of its buffering capacity at endosome pH, unfortunately; however, it induces cytotoxicity due to its high charge density. An alternative approach has involved combining (via electrostatic interactions) cationic liposomes with anionic, pH-sensitive polymers, to create a neutral delivery system that is both pH-sensitive and less cytotoxic. Environment (pH)-sensitive polymers such as poly (propyl acrylic acid) (PPAA) has been studied for their ability to enhance the delivery of plasmid DNA molecules into cells by its membrane lytic abilities at the endosome pH. Murthy et al. have demonstrated selective hemolysis effect induced by this polymer at the acidic pH, that of the endosomes, while absence of lysis at neutral or cytoplasmic pH [43]. Amongst the members of the family of acrylic acids including PMAA, PEAA, PPAA and PBAA, this property was unique to PPAA. Kyriakides et al. reported a 20-fold increase in β-galactosidase expression (*in vitro*) upon addition of PPAA, compared to control DOTAP/DNA lipoplexes [36]. This key feature allows for timely release of the cargo to the appropriate location within the cell. Hydrophilic polymers such as poly (ethylene oxide) (PEO) have been used to provide ‘stealth’ to the delivery system, thereby preventing interactions with hydrophobic serum nucleases.

1.3.3. Poly (alkylene oxide) polymers

In 1994, PEG-L-asparaginase (Oncospar; Enzon) was the first PEG nanoparticle therapeutic to receive FDA approval for the treatment of acute lymphocytic leukemia [44]. Other examples include PEG-interferon-alpha 2a (Pegasys, Roche and PEG-

interferon-alpha 2b for the treatment of hepatitis C [45]. Amphiphilic block copolymers have been utilized to improve plasmid DNA and antisense oligonucleotide delivery to a variety of tissues. Pluronics®, block copolymers of PEO and PPO, ensure protection of complexes from degradative serum proteins, while also inducing favorable interactions with the cell membrane, which promote entry of therapeutic cargo into cells (Fig.1.3) [46]. To utilize the beneficial properties of these polymers for intracellular delivery of genes, antisense oligonucleotides (ODNs), or siRNAs, several block (b) or graft (g) copolymers have been synthesized to create copolymers such as PEI-g-PEO and PEI-b-Pluronic [2, 37]. These examples demonstrate that graft or block copolymers, which are conjugates of polymers, can maintain the multiple functionalities of two or more polymer constituents.

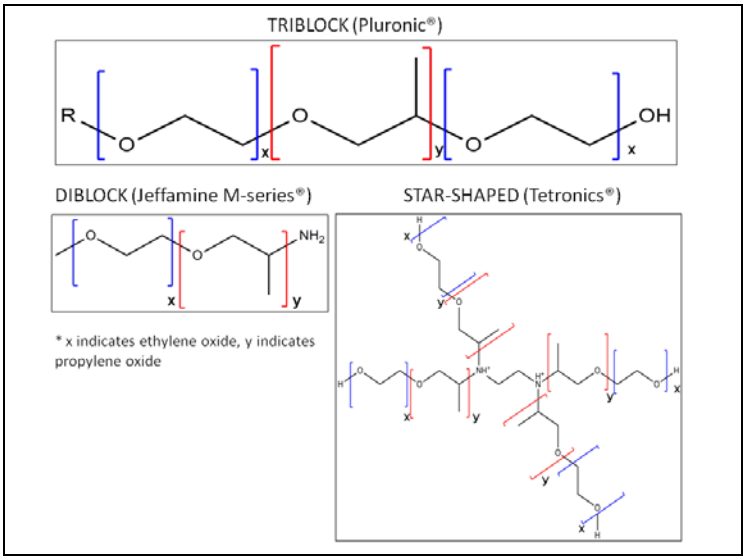

Figure 1.3: Chemical structure of Pluronics® with varying proportions of ethylene oxide (EO) and propylene oxide (PO) groups

Early studies by Liaw et al. [47] demonstrated ocular delivery of plasmid DNA using the non-ionic PEO-PPO-PEO copolymer. Several examples in literature have

demonstrated the use of Pluronic block copolymers for plasmid DNA delivery to target muscle dystrophy. The motivation for the use of Pluronics for this application is the inability of naked plasmid DNA to achieve significant levels of the expression that is necessary to achieve a therapeutic effect. Kabanov et al. introduced the use of Pluronics, a mixture of Pluronic L61 and Pluronic F127 (commercially known as SP1017), to aid in the intramuscular delivery of erthyropoietin encoding plasmid DNA to mice and rats with muscular dystrophy [48]. SP1017 was successful in enhancing gene expression by 10-fold in comparison to naked DNA. As a progression from linear triblock copolymers chemistry (also known as poloxamers), the family of tetrafunctional polymers called poloxamines, consisting of a center with an ethylenediamine unit and four PEO-PPO blocks, have emerged. Work by Pitard et al. introduced poloxamine 304, commercially known as Lutrol®, PEO 75-PPO 30-PEO 75, for plasmid DNA delivery to mouse muscle tissue [49]. This work motivated the design of carriers to include both polycations and pluronics for plasmid DNA delivery; thereby incorporating the advantages that each of these components has to offer. It was found that the more lipophilic copolymers, such as P85 [Hydrophilic Lipophilic Balance (HLB) of 16] or SP1017 (mixture of L61 and F127 with HLB of 20), were more effective compared to more hydrophilic polymers. Differences in polymer HLB values for PEO-g-PEI and P85-g-PEI have also affected in vivo biodistribution to the kidney or liver, respectively [50].

The P85-g-PEI transfection system proved to be efficient for Ku86 antisense oligonucleotide (AON) delivery in vivo human colon adenocarcinoma xenografts, where Ku86 is a gene implicated in tumorgenesis and tumor resistance. In comparison to PEI-AON complexes, PEI-Ku86 ASO complexes demonstrated high stability in serum-

containing solutions by reducing aggregation in the bloodstream, and also reducing toxicity effects [51]. This delivery system displayed significant inhibition of tumor growth when used in conjunction with ionizing radiation (IR), proving to be promising in a clinical setting.

1.4 Parameters for design of carrier chemistry

The physical properties of nanoparticles such as their size and charge, and properties of carriers (polymers or liposomes) such as their flexibility, membrane rigidity, surface architecture (PEG chain length and density of chains), dictate stability of the carrier in the bloodstream, in vivo biodistribution to organs, interaction of the carrier with the nucleic acid molecule, association of the carrier with the cell membrane and the ability to traffic intracellular degradative pathways. As discussed in previous sections, at the extracellular level, nucleic acid delivery barriers include opsonins, extracellular matrices, degradative enzymes, and phagocytes. While in the intracellular milieu, escape from endosomes before lysosomal degradation has been identified as a key barrier.

1.4.1 Physical parameter- Size

The size of nanoparticles is an important determinant of liposome fate in vivo. It is known that when free nucleic acid is injected into blood it is either instantly degraded by nucleases present in the blood or rapidly excreted through kidney filtration into urine because of its small size. In the case of a carrier, the first mechanical filtration barrier, the lung capillary bed, attracts larger, positively-charged particles, while neutral or negatively charged particles leave the lung and enter into systemic circulation to encounter all tissues [52]. The organs, liver, spleen and tumor, allow particles in the range of 200-300 nm [53]. The RES, as discussed earlier, consist of the macrophages of

the liver, spleen and bone marrow. The conjugation of PEG onto nanoparticles prevents the binding of opsonin proteins, which signal macrophage cells, called Kupffer cells in liver to stimulate particle degradation. Therefore, PEG was introduced to create a highly, solvated hydrophilic polymer layer to provide shielding from opsonins [54]. Finally, and most importantly for tumor delivery is the form of passive targeting called enhanced permeation retention (EPR) that has been discussed in previous sections. The EPR effect arises from the leaky vasculature of tumors that lack basement membrane, allowing 200 nm sized particles to enter and be retained at the diseased site because of a lack of lymphatic drainage [52, 55]

Liu et al. have extensively explored the fate of liposomes in the range 30-400 nm in the blood, liver, spleen and tumor by injecting mice with radioisotope-labeled liposomes by IV injection and examining accumulation in tissues after 4 hrs [56]. The key findings include retention of 60% of 100-200 nm-sized liposomes in the blood compared to 20% for 250 nm-sized particles. Further evidence indicates that 100-200 nm-sized particles showed 4 times more accumulation in the tumor compared to 300 nm-sized particles. Allen et al. found 10-20 fold increase in rate of tumoral uptake of 120 nm particles compared to 170 nm for small lung cancer [57].

1.4.2 Physical parameter- Charge

Arvizo et al. studied the effect of the surface charge of the nanoparticle by using neutral (TEGOH, zeta = -1.1mV), zwitterionic (Tzwit, zeta =-2.0mV), negative (TCOOH, zeta=-37.9mV) and positively-charged particles (TTMA zeta= +24.4.mV) to determine how this parameter affects circulation time of nanoparticles. For all these particles, two routes of administration, IV and IP, were studied. The results indicated

improved pharmacokinetics with neutral and zwitterionic particles (independent of the route of injection), which accumulated more efficiently into the tumor. After IV injection, the TCOOH accumulated in the tumor, while the positively-charged particle, TTMA, failed to do so [58]. Several reports support the fact that positively charged polymeric nanoparticles accumulate in the liver and spleen despite PEG functionalization. This study reinforces the benefit of neutral charged particles which achieve favorable biodistribution profiles, with higher accumulation to the diseased tumor site.

Levchenko et al. prepared liposomes of 200 nm with varying charges and studied their effect on tissue distribution in mice over a period of time. Here it was found that neutral liposomes (zeta = +/- 10mV) retained higher concentrations in the blood compared to negatively-charged liposomes [59]. And in the case of positively-charged particles, interaction with negatively-charged serum protein formed aggregates of large sizes that were directed to the liver and lung [60]. PEGylation improved problems of charge by creating a mask around the nanoparticle. Yamamoto et al. showed that anionic Tyr-Glu-PEG/PDLLA micelles displayed lower distribution (by 10 times) to the liver and spleen 4 hrs post-injection, and this was hypothesized to be a result of steric and electrostatic repulsion [61]. This work reinforces the positive effects of neutral and negatively-charged surface nanoparticles in terms of reduced adsorption of plasma proteins and elimination by RES triggered by macrophages.

1.4.3 Physical parameter- Hydrophilicity/Hydrophobicity

The importance of carrier hydrophobicity for favorable association with cell and endosome membranes has been established by several research groups. Wang et al. investigated amphiphilic modification of chitosan with varying hydrophobic LA (linoleic

acid) and hydrophilic PMLA (poly β-malic acid) [62]. An optimum degree of hydrophobicity was found where association with RBC model membranes and cellular uptake was observed. In this study, the experimental setup excluded the serum barrier, where the degree and presentation of hydrophilic groups plays a role.

Several groups have explored hydrophobic modifications to PEI, chitosan, PLL, and polycations such as dendrimers, DMAEMA and dextran-spermine, with the goal of increasing association with cell membranes, binding with pDNA and facilitating dissociation with pDNA [63]. It must be noted that polymers offer several advantages compared to liposomes because of relatively small size, narrow PDI, ease to modify chemistry, and high stability. However, lipid containing transfection reagents have enhanced compatibility with the plasma membrane, which can be seen by comparing commercially available lipid-reagents like Lipofectamine 2000 and INTERFERin, which are more efficient compared to polymer-based reagents such as jetPEI and Metafectene. The emergence of branched PEI (25 kDa) derivatives, such as PEI modified by oleic acid and stearic acid, tyrosine, and low molecular weight PEI modified with alkyl acrylates, have created more stable nanoparticles with increased silencing efficiency [64-66]. Bromberg et al. found that by attaching PPO-PEO polyether to PEI and guanidinylating the conjugate, an enhancement in transfection under serum conditions was observed [67]. Kabanov and Bromberg synthesized P123-g-PEI and Pluronic L92-pDMAEMA, respectively, with the addition of free P123 to these systems to cause even more enhanced transfection effects [68, 69]. One possible theory to explain the additional benefit of free P123 is the formation of small, stabilized particles, while the other involves the concept that free P123 binds to serum proteins, leaving the complex

unaltered or unaffected by serum proteins, and thereby allowing transfection to proceed in the presence of serum- without any hindrance.

Takahashi et al. designed a polyamidoamine dendron-based cationic lipid introducing two dodecyl chains, and observed efficient cell transfection with synergistic effect on endosome buffering and membrane fusion with the endosome [70]. Liu et al. measured the adsorption of a hydrophobized hyperbranched polyglycerol-PEG copolymer onto RBC. It was observed that plasma removed most of the bound hydrophobized polymers from RBCs, and albumin caused desorption of bound polymers from the cell membrane [56]. It is hypothesized that the hydrophobic portions of albumin interact with the hydrophobic polymers, dissociating the complexes, and affecting size and integrity of complexed nucleic acid.

Hydrophilic polymers such as poly (ethylene oxide) (PEO) have been used to provide ‘stealth’ to the delivery system, thereby preventing interactions with hydrophobic serum nucleases. Gref et al. were the first to introduce the advantages of pegylation on PLGA-PEG nanoparticles to increase blood residence time. It was found that the amount of protein absorbed on PLA-PEG 5kDa was reduced by ~ 80% for the optimum of 5 wt %, compared to PLA nanoparticles without PEG [71]. Nagayama et al. sought to understand the interaction of opsonins with PEG nanoparticles and further, that of the complex with macrophages in the liver. It was suggested that the rate of hepatic uptake of particles was mainly dictated by the process of opsonization. Of the complement proteins, protein C3 and immunoglobulin G (IgG) were adsorbed on nanoparticles resulting in increased uptake by Kupffer cells as shown by in vitro studies [72]. This same group showed that blood clearance of smaller-sized nanoparticles was twice as slow allowing

twice as much accumulation in the tumor, compared to larger sized particles. It must be noted that the PEG effect is transient, wherein eventually the process of opsonization and macrophage clearance will take place. To study the specifics of PEG grafting, research groups have explored effects of PEG molecular mass and graft density [73].

CHAPTER 2: MODIFICATION OF PH-SENSITIVE POLYMER, PPAA, FOR IMPROVED ANTSIENSE DELIVERY & IN VITRO GENE SILENCING EFFECT IN SERUM

2. 1 ABSTRACT

Antisense technology holds tremendous potential in the research and clinical settings. However, successful delivery of antisense oligodeoxynucleotides (ODNs) to the intracellular site of action requires the passage of many barriers, including survival against extracellular serum nucleases and escape from endolysosomal degradation. Previous work has shown that the effectiveness of antisense delivery by the cationic liposome, dioleoyl-3-trimethylammonium-propane (DOTAP), is enhanced substantially by the incorporation of a pH-sensitive polymer, poly (propylacrylic acid) (PPAA), in serum-free media. To improve this system for application in serum-containing media conditions, PPAA was modified in this work by grafting onto it either poly (ethylene oxide) (PEO) or a more hydrophobic analog, poly (oxyalkylene amine), known as Jeffamine. The ternary formulation of DOTAP/ODN/PPAA-g-Jeffamine resulted in 8-fold increased uptake of fluorescently-labeled ODNs compared to DOTAP/ODN/PPAA and ~80% silencing of green fluorescent protein (GFP) expression in CHO-d1EGFP cells treated in the presence of 10% FBS-containing media. In contrast, the carrier systems that contained PPAA or PPAA-g-PEO failed to display any significant antisense activity in the presence of serum, even though all of the delivery systems displayed moderate to high levels of antisense activity in serum-free conditions. The results reveal that the carrier system with the Jeffamine graft copolymer effectively mediates specific gene silencing in the presence of serum, while the system with the PEO graft copolymer fails

to do so. While the pH-dependent lytic functionality of PPAA was found to be lost upon grafting with PEO or Jeffamine, the hydrophobicity of the latter was sufficient to mediate cellular internalization and endosomal escape. Thus, the PPAA-g-Jeffamine copolymers hold substantial promise as agents for controlled therapeutic delivery of antisense oligonucleotides.

2.2 INTRODUCTION

Non-viral carriers such as cationic polymers, micelles, and liposomes have been studied extensively for their ability to bind with and deliver anionic antisense ODNs and short interfering RNA (siRNA) molecules into cells. Liposomes are composed of phospholipid bilayers that are similar to biological membranes, initiating intimate contact with and entry into cells. Liposomes of cationic nature, like DOTAP, bind with and encapsulate anionic molecules such as plasmid DNA, antisense oligodeoxynucleotides (ODNs) and short-interfering RNAs (siRNAs), and enter cells by fusion-mediated processes or endocytosis. Polymers, on the other hand, can be tailored with chemical functionalities for biological tasks.

The work presented here combines features from both systems through the use of hydrophobically modified, environmentally protective graft copolymers to enhance liposome-mediated delivery of antisense ODNs. Amongst the family of acrylic acid polymers consisting of PAA, PEAA, PMAA and PPAA, it has been found that PPAA demonstrates maximum membrane lysis at the acidic or endosome pH without lysis at neutral or physiological pH [36]. Once the drug or gene carrier is inside the endosomes of cells, this property of PPAA aids in releasing the endosome contents, thereby allowing

the therapeutic cargo to escape the endolysosomal track and reach the appropriate location within the cell [74]. Hydrophilic polymers, such as poly (ethylene glycol), provide “stealth” to drug or gene carrier systems, protecting them from serum nucleases and increasing the half-life of the drug [42, 75, 76]. Block or graft copolymers are designed to combine multiple functionalities to overcome delivery barriers at the extracellular and intracellular levels.

It has been established that a major barrier to the intracellular delivery of ODNs is their sequestration in endosomes, which eventually fuse with lysosomes, thereby leading to degradation of their contents. To overcome this barrier, the pH-sensitive anionic polyelectrolyte, poly (propylacrylic acid) (PPAA), was used as an adjunct to ODN carrier systems. PPAA has been shown to lyse membranes at endosomal pH (~ 5–6), while leaving membranes unperturbed at physiological pH (~ 7.2) [77]. This functionality of PPAA improved significantly the *in vitro* transfection efficiency of liposome-based complexes containing plasmid DNA [78]. Similarly, our research group has demonstrated successful *in vitro* antisense ODN delivery by utilizing PPAA in complexes of DOTAP/ODN. However, the delivery efficiency of these ternary complexes containing PPAA is reduced in treatment conditions involving serum-containing media.

Our strategy to improve the performance of the DOTAP/ODN/PPAA delivery system in the presence of serum involved modifying the chemistry of PPAA by grafting onto it hydrophilic poly(ethylene oxide), PEO, or poly(oxyalkylene amines), Jeffamine. PEO is known for its ability to increase the stability of drug and nucleic acid delivery vectors by providing protection against serum nuclease degradation and removal by the reticuloendothelial system [35, 75]. We hypothesized that the introduction

of a PPAA-grafted copolymer chain consisting of both EO and hydrophobic propylene oxide (PO) could improve the cell membrane penetration capability of complexes, while retaining the protective properties of the PEO that are required to provide stability in serum. Previous work by Kabanov and coworkers has demonstrated successful ODN delivery using poly (ethylene imine) (PEI) conjugated to Pluronics®, which are triblock copolymers in a PEO–PPO–PEO configuration [46, 48]. In this study we present a comparison of the effects of PEO- and Jeffamine-grafted PPAA copolymers on ODN delivery and antisense activity of ODNs targeted to silence the short half-life green fluorescent protein (d1EGFP) in a stably expressing Chinese hamster ovary (CHO) cell line.

2.3 MATERIALS AND METHODS

2.3.1 Materials

A phosphorothioate oligodeoxynucleotide tagged with Cy5 (5′-Cy5-TTG TGG CCG TTT ACG TCG CC-3′) was used for physical and biological studies. The presence of the Cy5 tag did not significantly alter the delivery of ODNs into cells or their ability to bind with mRNA and achieve an antisense effect [79]. This 20-mer oligonucleotide (ODN) (*EGFP157*), previously selected for down regulation of d1EGFP, was used to assess the degree of silencing or antisense effect. The ODNs were obtained from Integrated DNA Technologies (Coralville, IA) and delivered as HPLC grade. Before use, lyophilized ODNs were resuspended in phosphate buffer saline (PBS) (Invitrogen, Carlsbad, CA) at pH 7.2 to obtain a stock concentration of 100 μM.

The cationic liposomal formulation, N-[1-(2,3-dioleyloxy)propyl]-N,N,N-trimethylammonium methyl sulfate (DOTAP), was purchased from Roche Applied Science (Indianapolis, IN). Lipofectamine2000 was purchased from Invitrogen and used as directed. Poly(α-propylacrylic acid) (PPAA) (M_n = 27 kDa) was purchased from Polymer Source (Montreal, Canada). PEO monomethyl ether (MW = 5 kDa) was purchased from Fluka. 1-(3-dimethylamnopropyl)-3-ethyl-carbodiimide (EDCI) was purchased from Kawaguchi Chemical Industry Co., Ltd. (Tokyo, Japan). 4-(dimethylamino) pyridinium 4-toluenesulfonate (DPTS) was synthesized following a published procedure [80]. Jeffamine M-2070 (MW = 2 kDa, EO/PO = 31/10) was a gift from Huntsman International, LLC (Woodlands, TX).

PPAA polymer, which was received as a dried powder, was solubilized in 0.1 N NaOH in PBS (pH 13). The Jeffamine M 2070 grafted PPAA copolymer (PPAA-g-Jeffamine) was solubilized in a NaOH–PBS formulation (pH 12.5) and further diluted in PBS. The PEO grafted PPAA copolymer (PPAA-g-PEO) was solubilized directly in PBS (pH 7.4). Solutions of DOTAP, ODN and polymers were stored at 4 °C and vortexed prior to use. All other reagents and solvents were purchased from Sigma-Aldrich (St. Louis, MO), unless noted otherwise. All buffers were prepared in MilliQ ultrapure water and filtered (0.22 μm) prior to use.

2.3.2 Graft copolymer synthesis

The synthesis procedure of the graft copolymers was similar to previously described methods for the synthesis of similar polyacrylate-grafted PEO and Jeffamine comb copolymers [80, 81]. For the PPAA-g-PEO copolymer, 200 mg PPAA was added to 5 ml DMSO along with 11 mg 4-(dimethylamino) pyridinium 4-toluenesulfonate

(DPTS), and a slight molar excess of PEO monomethyl ether required to achieve the target graft ratio. The mixture was stirred for 30 min at room temperature, after which 41 mg 1-(3-dimethylamnopropyl)-3-ethyl-carbodiimide (EDCI) was added. The reaction was allowed to proceed at room temperature and driven to completion with subsequent 100 mg aliquots of EDCI added on days 4, 9, and 11. The reaction mixture was then transferred to a Slide-A-Lyzer cassette with 10 kDa MW cut off and dialyzed exhaustively against deionized water. The dialyzed solution was then lyophilized.

For the PPAA-g-Jeffamine copolymer, the same synthesis, dialysis and lyophilization protocols that were used for the PPAA-g-PEO copolymer were followed, with the exception that Jeffamine M-2070 replaced the PEO monomethyl ether and 1-hydroxy-1H-benzotriazole (HOBt) was used as the catalyst in place of DPTS. The extent of PEO and Jeffamine M-2070 grafting onto PPAA backbones was determined by NMR spectroscopy, which was performed on a Varian 400 MHz spectrometer. The percentage of grafting was calculated by the ratio of the integrated peak areas of the methylene protons in the grafted chains to the methyl protons in PPAA. For the PPAA-g-PEO: ^{1}H NMR (DMSO-d_6) δ 0.80 (s, CH_3), 0.95–2.0 (m, br, CH_2(PPAA)), 2.10(br), 2.17 (br), 2.29 (br), 2.35, 2.41, 2.64, 2.77, 2.9–3.3 (br), 3.2 (OCH_3), 3.29 (t), 3.47 (s, –OCH_2CH_2O–), 3.65 (t), 4.10 (br, C(O)OCH_2CH_2OPEO), 4.6–4.8 (br), 4.9–5.2 (br), 7.05 (br), 8.45 (br). For the PPAA-g-Jeffamine: ^{1}H NMR (DMSO-d_6) δ 0.82 (s, CH_3), 1.0–2.0 (br, CH_2), 2.10, 2.17, 2.2–3.0 (br), 2.9–3.0 (br), 3.2 (OCH_3), 3.24–3.42 (m, CH + CH_2(PPO)), 3.47 (s, –OCH_2CH_2O–), 3.50, 3.51, 3.52, 3.65 (t), 4.6–4.8 (br), 5.0–5.3 (br), 5.50 (s), 7.08 (d), 7.45–7.60 (br), 7.66 (C(O)NH). Conventional gel permeation chromatography was used to monitor the progress of the reactions and determine the final molecular weight and

polydispersity of the graft copolymers. This was performed with the Waters 510 HPLC unit equipped with a Waters 410 Differential Refractometer, a 5 μm PL gel precolumn, and two PL gel columns (pore size 10^3–10^5 Å) that have been calibrated with polystyrene standards by using DMF containing 0.1% trifluoroacetic acid as the mobile phase at a flow rate of 0.8 ml min^{-1}.

Scheme 1: Modification of poly (propyl acrylic acid) (PPAA) chemistry by grafting poly (ethylene oxide) (PEO) or its analog poly (ether amine), commercially known as Jeffamine (EO: PO of 10:31) to create PPAA-g-PEO and PPAA-g-Jeffamine copolymers

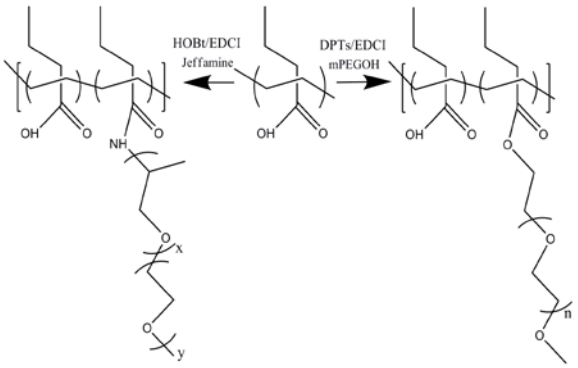

2.3.3 Preparation of DOTAP/ODN/Polymer Complexes

The delivery vectors were self-assembled from their components by electrostatic interactions, first between the cationic DOTAP liposomes and anionic ODN, and then between the DOTAP/ODN complexes and the anionic polyelectrolytes (PPAA, PPAA-g-PEO or PPAA-g-Jeffamine). Complexes were prepared using a DOTAP/ODN weight ratio of 10:1, which corresponded to a charge ratio of 4.7 (+/−). The net charge ratio is defined as the ratio of the moles of DOTAP amine groups to the sum of the moles of ODN phosphate groups and PPAA carboxylic acid groups. The DOTAP working

concentration was 20 μg/ml (as recommended by Roche). All DOTAP/ODN/polyelectrolyte complexes were formed by mixing equal volumes of DOTAP and ODN, followed by incubation for 30 min at room temperature. Polyelectrolyte was then added to the DOTAP/ODN solution to produce the desired net charge ratio, and incubated for an additional 30 min at room temperature. DOTAP and ODN were assumed to be completely ionized (100%), while the carboxylic acids of PPAA were assumed to be 33% ionized at pH 7.4 based on its pKa value [36]. This assumption was also used to determine the ionization degrees of the carboxylic acid groups in PPAA-g-PEO and PPAA-g-Jeffamine copolymers. LipofectAMINE 2000 (Invitrogen, Carlsbad, CA), the control delivery agent, was complexed to ODN in a weight ratio of 2:1. The ratio of complex volume to buffer/media volume was maintained constant at 1:4.

2.3.4 Measurement of Antisense ODN encapsulation

The degree of ODN encapsulation in the vectors was quantified by measuring the fluorescence quenching from Cy5 labeled ODNs (F-ODNs). Solutions of DOTAP/F-ODN in the presence of PPAA or PPAA graft copolymers were loaded into a polystyrene clear bottom 96-well black plate (Corning, Corning, NY) (F-ODN concentration = 750 nM). The Cy5 fluorescence intensity was measured at excitation and emission wavelengths of 646 and 680 nm, respectively, using an Ascent Fluorescence Multi-well Plate Reader (Thermo Electron Corporation). After background subtraction each data point was normalized to control (uncomplexed ODN). Disruption of the complexes to recover encapsulated F-ODN was achieved by using a 0.25% solution of Triton X-100. Negligible fluorescence (close to that of background) was obtained for carrier (in the

absence of ODN) and Triton X-100 (in the absence of ODN and carrier). The degree of encapsulation was calculated by the formula:

$$\% \text{ Encapsulation} = \frac{(F_{680,sample} - F_{680,PBS})}{(F_{680,ODN} - F_{680,PBS})} * 100$$

2.3.5 Particle sizes and zeta potential measurements

Complexes were prepared by first mixing DOTAP and ODN solutions (final ODN concentration 300 nM, DOTAP/ODN charge ratio 4.7), followed by the addition of polyelectrolyte (PPAA, PPAA-g-PEO or PPAA-g-Jeffamine) to yield a net charge ratio within the range of 3 to 0.25. All solutions of DOTAP, ODN and polymers were diluted in PBS. The ratio of complex volume to buffer (PBS, Opti-MEM, or MEM) volume was maintained at 1:4. Complexes were analyzed using a Malvern Instruments Zetasizer Nano ZS-90 instrument (Southboro, MA) with reproducibility being verified by collection of sequential measurements. DLS measurements were performed at a 90° scattering angle at 25 °C. DLS and *z*-average sizes were collected and analyzed immediately after the formation of DOTAP/ODN/polyelectrolyte complexes (total incubation time of 60 min).

2.3.6 Hemolysis and Pyrene fluorescence assay

The ability of PPAA and the grafted polymers to disrupt membranes was assessed using a hemolysis assay. Solutions of PPAA, PPAA-g-PEO and PPAA-g-Jeffamine were added to pH buffers 5.0, 5.5, 6.0, 6.5 and 7.0 at 40, 240 and 400 µg/ml and vortexed thoroughly. These various amounts of polymer corresponded to equivalent moles of carboxylic acid groups. To these polymer solutions, fresh RBCs that had been washed three times with 100 mM NaCl were added at a concentration of 10^8 cells/ml, incubated in a waterbath at 37^oC for 1 hr, and then centrifuged for 4 min at 400 *g* to pellet the intact

RBCs. The absorbance of the supernatant (541 nm) was determined on a UV spectrophotometer. Experimental controls included RBCs in pH buffers in the absence of polymer (negative control) and RBCs in distilled water (positive control).

Pyrene was used as a hydrophobic fluorescent probe to assess environmental polarity of polymer and graft copolymer solutions. The polymer stock solutions were diluted with phosphate buffer solution of various pHs from 5.0 to 7.4 to yield a final polymer concentration of 1 mg/ml. Pyrene was added to each sample at a final concentration of 10^{-7} M. Emission spectra of pyrene was recorded on a spectrofluorometer (excitation at 335 nm) at room temperature and the intensities of emission peaks at 382 and 392 nm were recorded.

2.3.7 Antisense ODN delivery and gene silencing

Cells were seeded onto 12-well plates at 10^5cells/ml (with 1 ml volume per well) ~18 h prior to ODN treatment. For cellular uptake and antisense studies, cells were treated with Cy5-labeled antisense ODN (targeting d1EGFP) at a final ODN concentration of 300 nM per well. In the case of treatment, 200 μl of complexes were prepared, mixed with either Opti-MEM serum-free or 10% FBS-containing medium and added to each well. For control samples, complexes were substituted with 200 μl of PBS. After 4 hours of cell exposure to treatment, medium containing complexes was aspirated and replaced by fresh medium. Cells were assayed for Cy5-ODN uptake and GFP activity 24 hrs post-ODN treatment using fluorescence activated cell sorting (FACS).

Cells were prepared for FACS analysis first by washing with PBS buffer, followed by the addition of trypsin-EDTA to remove cells from the plate surface. Immediately after cell detachment, cell culture medium was added to neutralize the

trypsin. Next, cells were collected in pellet form by centrifugation for 3.5 min at 200 *g*, resuspended in 150 µl of PBS and maintained on ice until the time of analysis. Cells were analyzed for size (side scatter), granularity (forward scatter), intensity of Cy5 fluorescence (FL4 channel) and intensity of GFP (FL1 channel). Geometric mean fluorescence intensities for 10,000 cells were determined on the FACS Calibur three-laser flow cytometer. CellQuest software was used to acquire and analyze results. The degree of silencing was calculated from the GFP fluorescence of treatment samples normalized to control (untreated cells). The background GFP fluorescence from cells lacking d1EGFP plasmid was negligible.

2.3.8 Fluorescence Microscopy

Complexes were formulated as previously described using an anti-GFP ODN sequence labeled with a Cy5 fluorophore at the 5' end. CHO-pd1EGFP cells were seeded onto a Lab-Tek chamber at 25,000 cells/well in 300 µl of complete growth medium and cultured overnight. Cells were treated with complexes in 10% FBS-containing media. GFP fluorescent cells were visualized at 40X magnification using a Nikon microscope. Cy5 fluorescence was detected using excitation at 633 nm, and light emission at 663 to 738 nm emission. Green fluorescence was visualized at 488 nm excitation, and light emission at 500-555 nm emission.

2.3.9. Cytotoxicity assay

CHO-d1EGFP cells were seeded onto a 96-well plate and treated with 20 µl of complexes, prepared according to methods described above, and mixed with 80 µl of 10% FBS-containing media. After 4 hrs of exposure to treatment, complexes were aspirated from wells and cells were replenished with fresh media. After 24 hrs, 20 µl of

MTS reagent (Promega, Madison, WI) was added to 100 µl of media, per the manufacturer's protocol, and cells were incubated for a period of 2 hrs under humidified conditions. The reduction of MTS tetrazolium into a coloredformazan product by the cells was quantified colorimetrically to represent cell metabolic activity. Metabolic activity was calculated from recording the absorbance (at 490 nm) of treatment samples normalized to control (untreated cells).

2.3.10 Statistics

Groups from gene silencing and cell viability experiments were compared using the one-way ANOVA test, and results were represented as mean ± standard deviation. Pair-wise comparisons between the various polymer-containing delivery systems were made using a Tukey HSD post-hoc test; a *p*-value less than 0.05 indicated significant difference compared with the control, as indicated by asterisks on the figures.

2.4 RESULTS

2.4.1 Synthesis and characterization of graft copolymers

The set of copolymers was synthesized by grafting either poly (ethylene oxide) monomethyl ether (PEO, MW = 5 kDa) or Jeffamine M-2070 monomethyl ether (Jeffamine, MW = 2 kDa) onto the backbone of poly (propylacrylic acid) (PPAA, MW = 27 kDa). The reactions were performed using carbodiimide coupling to yield graft copolymers with target graft densities from 1 to 25 mol% (Scheme 1). The grafting reactions were confirmed by ^{1}H NMR spectroscopy and GPC. The NMR spectra of PPAA-g-PEO copolymer contained chemical shifts expected for methylene protons of the PEO ester moiety formed by reaction of the PPAA carboxylic acids with the primary

alcohol of PEO (4.1 ppm). In the case of PPAA-g-Jeffamine, the spectra contained the amide proton (NH) that is formed by reaction of PPAA carboxylic acid groups with the primary amine of Jeffamine (7.6 ppm). The GPC chromatograms of the isolated products also revealed the disappearance of the starting materials and the appearance of new multimodal peaks at high molecular weight.

Only a few of the graft copolymers from the initial set synthesized were soluble in aqueous buffer, even when NaOH was added to enhance solubility. Hence, the physical and biological studies presented here are limited to a comparison of two similar graft copolymers that were soluble in aqueous buffer: 1) PPAA-g-PEO containing 21 mol% grafting of the 5 kDa PEO monomethyl ether, total number-average molecular weight of 57 kDa, and polydispersity index of 1.4; and, 2) PPAA-g-Jeffamine containing 25 mol% grafting of the 2 kDa Jeffamine M-2070, total number-average molecular weight of 58 kDa, and polydispersity index of 1.9. These two graft copolymers provided us with sufficient structural similarities to evaluate the relative effects of PEO and Jeffamine chains on the delivery of ODNs to cells in the presence of serum-containing treatment conditions.

2.4.2. pH-dependent hemolysis and pyrene fluorescence

To understand the effect of alkylene oxide grafting on the lytic properties of PPAA, the ability of PPAA, PPAA-g-PEO and PPAA-g-Jeffamine to disrupt erythrocyte (RBC) membranes was evaluated by quantifying the release of hemoglobin from RBCs spectroscopically. Solutions of PPAA, PPAA-g-PEO and PPAA-g-Jeffamine were prepared in pH buffers ranging from 5.0 to 7.0 at polymer concentrations of 40, 240 and 400 μg/ml, respectively, which corresponded to equivalent

moles of carboxylic acid groups in the polymers. PPAA produced significant hemolytic activity between the pH of 5.5 and 6.5, with maximum effect at pH 6.0 (which is the pH of the endosome) and a minimum hemolytic effect at pH 5.0 and 7.0 (Fig. 2.1A), consistent with previous work by Murthy et al. [77]. In comparison, the graft copolymers, PPAA-g-PEO and PPAA-g-Jeffamine, displayed low levels of hemolytic activity throughout the pH range of 5.0 to 7.0.

The environmental polarity of the polymers used in this work was monitored by measuring the steady-state fluorescence of pyrene. The emission spectrum of pyrene displays peaks at 371 and 392 nm, and an additional peak at 382 nm that appears only in the presence of a hydrophobic environment. The ratio of pyrene emission intensity at 382 nm to that at 392 nm was used to quantify the degree of polymer hydrophobicity in the various pH environments. The peak at 382 nm was absent for pyrene solution in the absence of polymer (control) and for pyrene solutions in the presence of PEO (ungrafted) or Jeffamine (ungrafted), which each failed to display any hydrophobicity throughout the pH range. PPAA binding of pyrene is consistent with a conformational shift from an expanded, hydrophilic coiled polymer at neutral pH to a more compact, globular structure at acidic pH [82]. The pH value at which the ratio of I_{382}/I_{392} is a maximum was 5.5 (Fig. 2.1B). This pH-dependent hydrophobic effect of PPAA is responsible for its hemolytic activity at acidic pH (Fig. 2.1A). The graft copolymers, PPAA-g-PEO and PPAA-g-Jeffamine, also resulted in pyrene emission enhancement, however, independent of the pH environment. Throughout the pH range, PPAA-g-Jeffamine demonstrated greater hydrophobicity compared to PPAA-g-PEO,

consistent with the presence of hydrophobic propylene oxide groups in PPAA-g-Jeffamine.

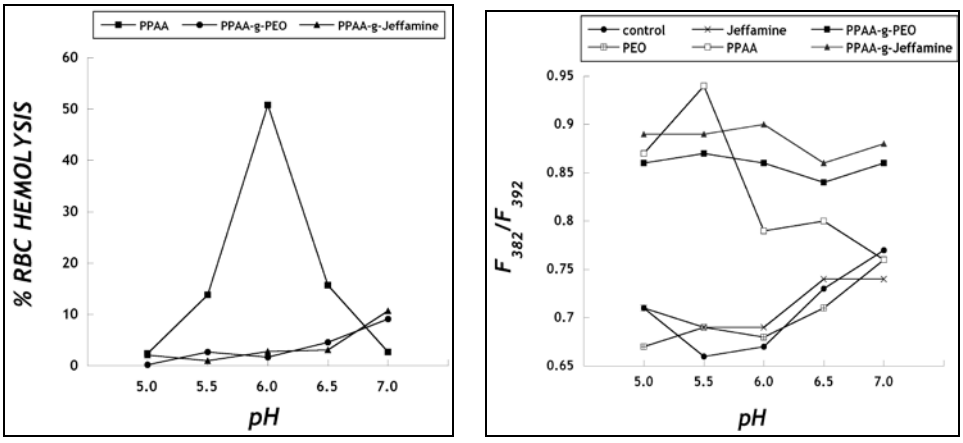

Figure 2.1: (A) Hemolysis induced by PPAA and graft copolymers **(B)** Ratio of pyrene intensities to indicate polymer hydrophobicities in various pH microenvironments

2.4.3. Antisense ODN encapsulation in complexes

The association between the cationic liposome, DOTAP, and anionic ODNs in the presence of the graft copolymers was determined by quenching of fluorescence from Cy5-labeled ODN (Table 2.1). The technique of using Cy5-labeled ODNs to quantify encapsulation of ODNs within a carrier has been performed earlier [83]. The detection of Cy5 fluorescence is indicative of free (unencapsulated) ODN that is either surface-bound or exposed to nucleases, or ODN that is free in solution, while encapsulated ODN is quenched and therefore undetectable. In this binding study, the charge ratio of DOTAP/ODN (+/-) in all the complexes was 4.7, and the net charge ratio of complexes with PPAA or the graft copolymers was 1. The degree of free ODN that is detected from

these complexes was less than 20%. The complexes containing PPAA and PPAA-g-Jeffamine maintained association with DOTAP/ODN more efficiently compared to those with PPAA-g-PEO ($p < 0.05$). Further, the encapsulated ODN was recovered when the complexes were disrupted with Triton X-100 surfactant. Overall, these results demonstrated that the binding ability of the cationic liposome, DOTAP, with anionic ODN is not altered drastically by the addition of PPAA or graft copolymers, and furthermore that the ODN associated with these complexes can be recovered.

SAMPLE (+ODN)	**% FREE ODN**	**% FREE ODN AFTER TRITON-X**
DOTAP	15.5 ± 1.6	84.7 ± 7.2
DOTAP/PPAA	8.4 ± 1.3	96.3 ± 15.3
DOTAP/PPAA-g-Jeffamine	9.4 ± 1.3	86.6 ± 18.3
DOTAP/PPAA-g-PEO	15.7 ± 1.8	90.0 ± 4.9

Table 2.1: Degree of ODN encapsulation by DOTAP/ODN complexes containing polyelectrolytes: PPAA, PPAA-g-PEO and PPAA-g-Jeffamine. Fluorescence (Cy5) corresponds to free Cy5-ODN in solution, while absence of fluorescence indicates quenching or ODN in bound (complexed) state.

2.4.4. Particle sizes and surface charge

The polymers and complexes were examined using the Zetasizer dynamic light scattering function (Fig. 2.2). The particle sizes of the free polymers at concentrations

used to prepare complexes for cell experiments were found to be below the detection limit. Particle sizes were measured at a fixed DOTAP/ODN charge ratio of 4.7, and DOTAP/ODN/polyelectrolyte charge ratio of 1, in PBS, Opti-MEM (reduced serum) and MEM (containing 10% FBS). The particle sizes of all complexes either in the absence or presence of PPAA, PPAA-g-PEO and PPAA-g-Jeffamine were found to be independent of the buffer solution. The particle size distribution of the complexes yielded a single peak that is indicative of the size of the complexes alone. Particle size measurements were obtained for a period of 10 mins to indicate particle stability and data runs were averaged. The complexes formed stable particles in each of the three buffer solutions with sizes ranging from 215-300 nm, and no statistically significant effect of the added polymers was observed (Fig. 2.2A). Overall, these observations are in agreement with the results from the ODN encapsulation studies, where all the complexes bind to ODN with equal efficiency. Further, they indicate that neither PPAA nor its graft copolymers induced widespread aggregate formation or flocculation, despite the overall charge neutrality of the system.

Since PPAA and its graft copolymers are charged species, their incorporation into DOTAP/ODN complexes was monitored by measuring changes in their zeta potential. A progressive decrease was observed in the zeta potential of DOTAP/ODN complexes upon addition of increasing amounts of anionic polymer or graft copolymer (Fig. 2.2B). Furthermore, as might be expected, the zeta potential of these complexes is close to 0 mV when the net charge of the polyelectrolyte mixture was neutral (N/P = 1). In the cases of PPAA and PPAA-g-Jeffamine, the decrease in zeta potential was marked compared to

PPAA-g-PEO. Overall, this result confirms the integration of these polymers into DOTAP/ODN complexes.

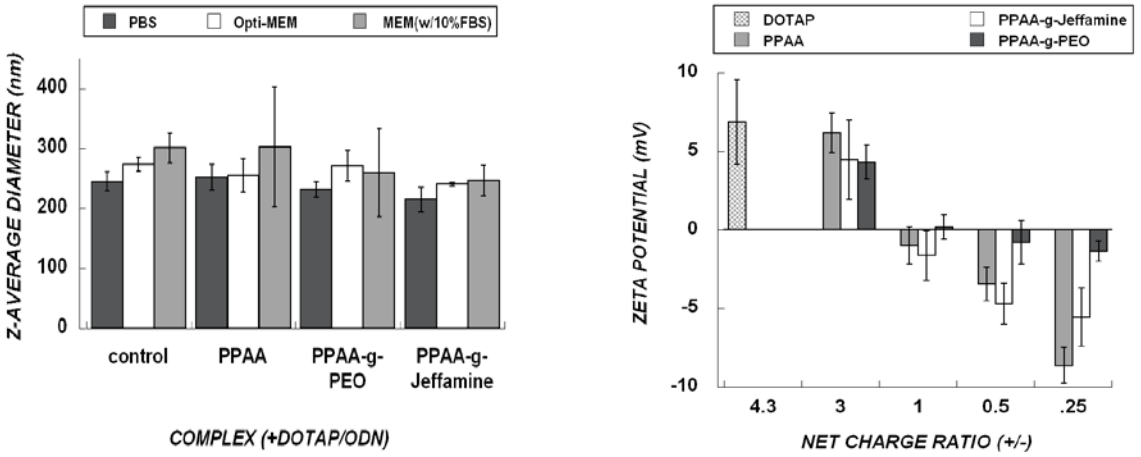

Figure 2.2: (A) Mean hydrodynamic diameter of DOTAP/ODN complexes alone ("control") or containing the indicated polyelectrolyte, in various buffer solutions. (B) Zeta potential of complexes of DOTAP/ODN "DOTAP" in the presence of increasing amounts of polyelectrolytes indicated as "PPAA", "PPAA-g-Jeffamine" and "PPAA-g-PEO" in the range of net charge ratios from 3 to 0.25.

2.4.5. Intracellular gene silencing in non-serum

The biological activity of the ODN complexes was assessed in CHO cells that stably express the gene encoding d1EGFP. The short intracellular half-life of the protein encoded by pd1EGFP gene provides a tight temporal coupling between pd1EGFP gene silencing at the mRNA level and fluorescence of GFP protein [74]. The intracellular delivery of ODN molecules into cells and the gene silencing effects were quantitatively determined from the fluorescence of Cy5-labeled ODN and d1EGFP expression,

respectively, using flow cytometry. Under serum-free media conditions, DOTAP mediated sufficient ODN delivery that produced moderate silencing of d1EGFP, but the inclusion of PPAA mediated greater silencing of GFP expression. Substitution of PPAA with PPAA-g-Jeffamine produced less gene silencing and with PPAA-g-PEO significantly less (Fig. 2.3) (p-value < 0.05 for PPAA-g-PEO vs. PPAA). Nonetheless, in serum-free medium, all of the delivery systems resulted in at least moderate levels of gene silencing.

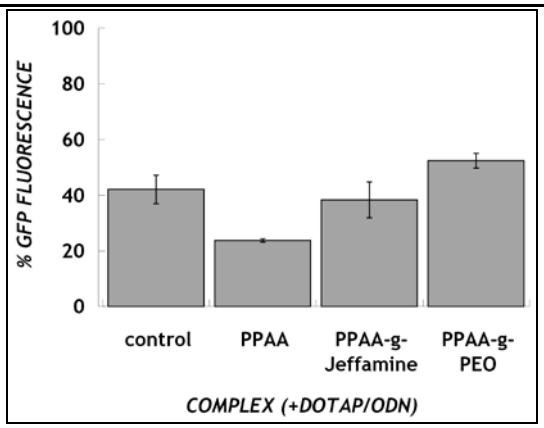

Figure 2.3: Silencing of target d1EGFP expression induced by various DOTAP formulations in serum-free medium. CHO-d1EGFP cells received 300 nM ODN treatment for a period of 4hr in the absence of serum, and were assayed 24 hours post-treatment. The "control" treatment refers to DOTAP/ODN (charge ratio 4.7) in the absence of polymer, and all other groups refer to the polymer that is added to this combination (to a net charge ratio of 1). GFP Fluorescence is normalized to untreated cells (100%). Data represent mean ± s.d. (n=3).

2.4.6. Intracellular ODN delivery and gene silencing in serum

For treatments in the presence of 10% FBS, however, relatively low levels of Cy5-ODN uptake and minimal antisense activity were induced by the DOTAP/ODN and DOTAP/ODN/PPAA systems over the range of charge ratios from 4 to 0.25, corresponding to increasing amounts of PPAA (Fig. 2.4 A,B). Taken together with the serum-free data, this result suggests that the presence of serum in treatment media hinders the intracellular uptake of ODN in complexes containing PPAA. Under similar treatment conditions with 10% FBS, the incorporation of PPAA-g-PEO copolymer into DOTAP/ODN complexes failed to increase intracellular ODN levels, which resulted in

insignificant antisense activity throughout the range of charge ratios tested (Fig. 2.4 B). In marked contrast, DOTAP/ODN complexes containing PPAA-g-Jeffamine copolymer produced an 8-fold increase in intracellular levels of ODN compared to DOTAP/ODN/PPAA in the presence of serum (Fig. 2.4A). This enhanced uptake with PPAA-g-Jeffamine correlated with a gene silencing effect of ~80% (Fig. 2.4B). These results imply that PPAA-g-Jeffamine is able to mediate both serum avoidance and membrane penetration. Moreover, complexes with PPAA-g-Jeffamine produced a greater antisense effect than those utilizing the commercial standard, Lipofectamine 2000. PPAA-g-Jeffamine-containing complexes were active over a range of net charge ratios from 2.0 to 0.25, where maximum ODN delivery and gene silencing effects were observed at the net charge ratio of 0.5.

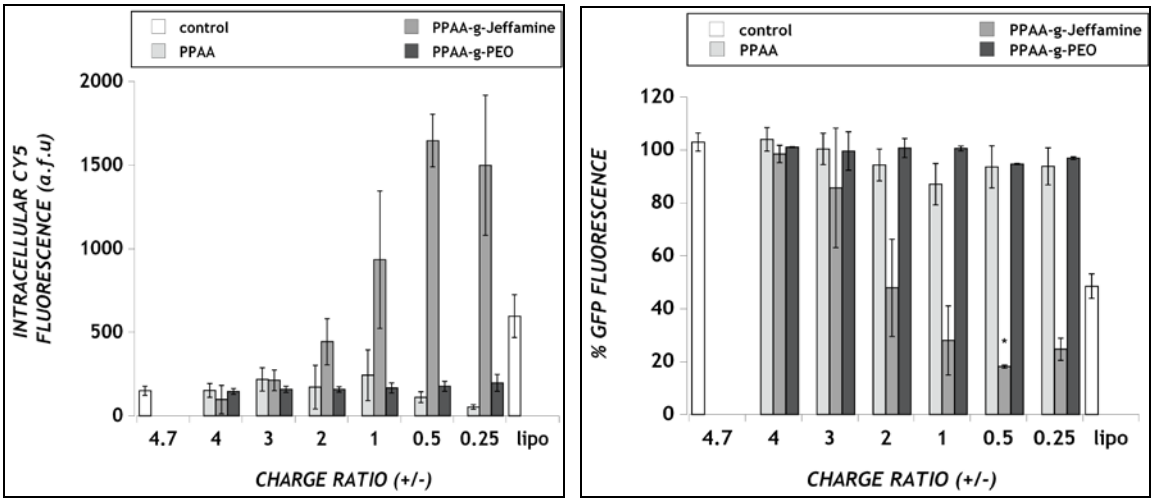

Figure 2.4: Cellular uptake of ODNs (A) and inhibition of target d1EGFP expression (B) in serum-containing medium. CHO-d1EGFP cells received 300nM ODN treatment in the presence of 10% FBS and were assayed 24 hours post-treatment. "Control" refers to DOTAP/ODN in the absence of polymer and all other groups refer to the polymer that is added to this combination. "Lipo" refers to delivery of ODN using Lipofectamine2000. In panel B, the % GFP Fluorescence is normalized to untreated cells (100%). Asterisk in (B) represents statistical significance ($p<0.05$) between the delivery systems at the charge ratio of 0.5. Data represent mean ± s.d. (n=3).

2.4.7. Fluorescent Images of intracellular antisense delivery and gene silencing in serum

To assess the intracellular distribution of ODNs and their relationship to gene silencing, treated CHO-d1EGFP cells were imaged using fluorescence microscopy (Fig 2.5). This figures shows Cy5 uptake (red) and d1EGFP fluorescence (green) in the various delivery formulations: (A) vehicle buffer, (B) ODN only, (C) DOTAP/ODN (+/-

=4.7), (D) DOTAP/ODN/PPAA (+/- =1), (E) DOTAP/ODN/PPAA-g-PEO (+/- =1) and (F) DOTAP/ODN/PPAA-g-Jeffamine (+/- =1). The PPAA-g-Jeffamine-containing delivery system displays Cy5-ODN distribution in almost all cells, indicating successful ODN delivery, and minimal green fluorescence, indicating successful gene silencing effect. These results confirm the results from flow cytometry as indicated in Figure 2.4.

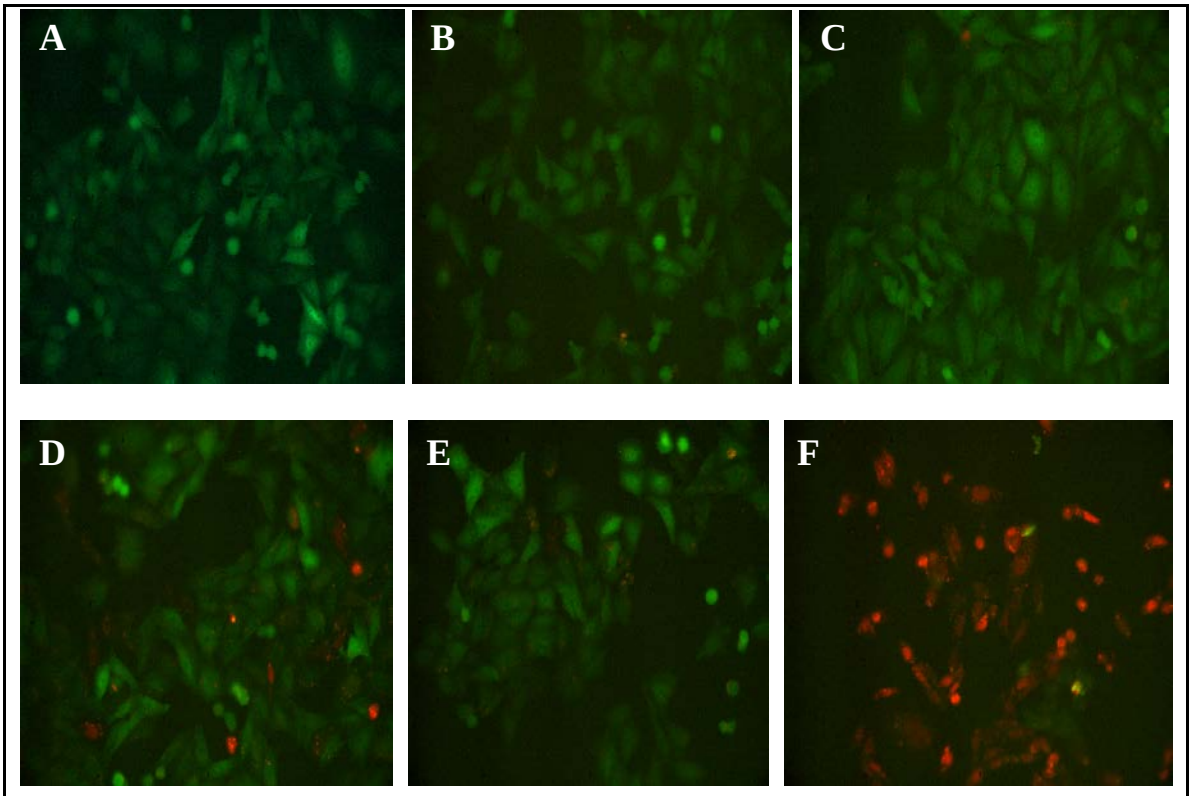

Figure 2.5: Fluorescent images of CHO-d1EGFP cells treated with (A) vehicle buffer, (B) ODN only, (C) DOTAP/ODN (+/- =4.7), (D) DOTAP/ODN/PPAA (+/- =1), (E) DOTAP/ODN/PPAA-g-PEO (+/- =1) and (F) DOTAP/ODN/PPAA-g-Jeffamine (+/- =1). Cells were treated with 300 nM final concentration of Cy5 (red) labeled ODNs for 4 hr under 10% FBS-containing cell culture media, after which they were washed and used for microscopy (24 hrs post-treatment).

2.4.8. Cytotoxicity

The use of polymeric carrier systems to enhance nucleic acid delivery has generally been accompanied by significant levels of cell death and/or impairment of cellular function [2, 84]. In order to test the cytotoxicity induced by these novel delivery systems, cell metabolic activity was quantified 24 hr post-treatment using a standard MTS assay. Increasing amounts of PPAA polymer to DOTAP/ODN complexes increased toxicity, with lowest cell metabolic activity (~ 55%) at the charge ratio of 0.25. In general, comparable levels of toxicity are observed when PPAA is replaced by PPAA-g-Jeffamine (Fig 2.6). In comparison, the least effective polymer, PPAA-g-PEO, induced negligible toxicity throughout the range of charge ratios tested, consistent with the idea that the presence of PEO resists cellular interactions.

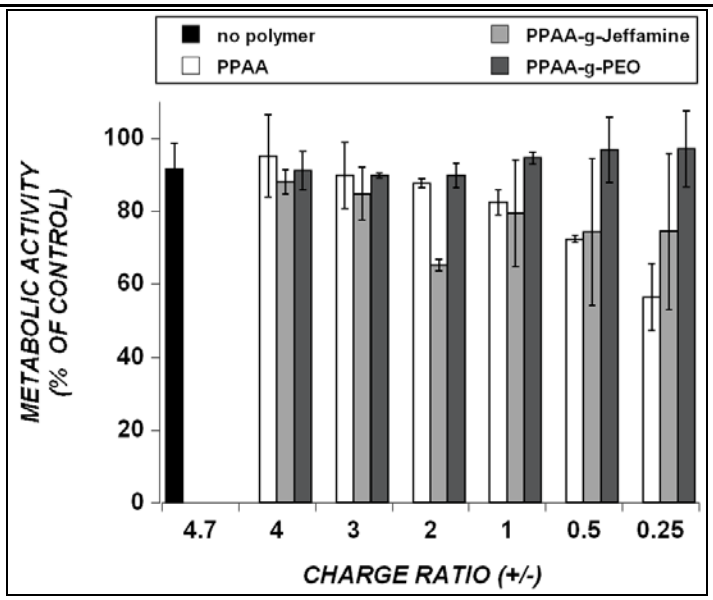

Figure 2.6: Effect of polyelectrolyte-containing complexes on CHO-d1EGFP cell metabolic activity, measured by the MTS assay. "No polymer" treatment refers to DOTAP/ODN (charge ratio 4.7) in the absence of polymer, and all other groups refer to the polymer that is added to this combination. Addition of increasing amounts of polymer to DOTAP/ODN complexes is indicated by charge ratios from 4 (lowest polymer concentration) to 0.25 (highest polymer concentration). Cells were treated with 300 nM ODN for 4 hr, in 10% FBS-containing cell culture media, and assayed 24 hr post-treatment. Data represent mean ± S.D. (n = 3).

2.5. DISCUSSION

The delivery of antisense oligonucleotides (ODNs) into cells is impeded severely by a variety of extracellular and intracellular barriers. An efficient carrier system must associate with ODN molecules to form stable particles, resist attack from serum proteins present in the bloodstream/media, enter the target cell by means of an efficient uptake route, and finally be able to escape the endosomes in order to avoid being trafficked to the degradative lysosomes. Previous work has shown that the inclusion of poly (propylacrylic acid) (PPAA), an anionic polymer with lytic abilities exclusively at endosomal pH, has improved the cellular delivery of ODN mediated by DOTAP liposome [74]. However, this system failed to display any significant antisense activity in CHO (Chinese Hamster Ovary) cells that were treated in the presence of 10% FBS. We have, therefore, modified PPAA to create graft copolymers containing hydrophilic or amphipathic moieties, based on the hypothesis that these structures would resist serum attack and possibly aid in delivery across cell membranes. Specifically, the backbone structure of PPAA was modified by grafting poly(ethylene oxide) (PEO) or Jeffamine (31:10 mole ratio of ethylene oxide to propylene oxide groups) at 21 and 25 mol% graft densities, respectively.

The results raise the interesting question of why there exist differences among the PPAA, PPAA-g-Jeffamine and PPAA-g-PEO-containing complexes in their ability to mediate cellular delivery of ODNs and initiate an antisense effect. The formation of the ternary delivery system from its individual components is driven by electrostatic interactions between: (1) the cationic liposome, DOTAP, and anionic ODN molecules and, (2) the resulting DOTAP/ODN complex and anionic polymers: PPAA, PPAA-g-

PEO or PPAA-g-Jeffamine. A fluorescence quenching assay demonstrated that the addition of PPAA, PPAA-g-PEO, or PPAA-g-Jeffamine to the DOTAP/ODN complexes did not affect the ability of DOTAP to maintain association with anionic ODN molecules, even when the net charge ratio was neutral. Moreover, it is noteworthy that the sizes of DOTAP/ODN complexes in the presence of any of the polymers are quite stable in a variety of buffer solutions ranging from PBS, Opti-MEM (reduced serum medium) and MEM containing 10% FBS. Furthermore, micellization of the free polymers was not observed by light scattering. Thus, it appears that the inhibitory effects of serum occur by modulating carrier-cell interactions, perhaps by competitive adsorption to cell membrane proteins, rather than by "attacking" the delivery vector directly.

PPAA and its graft copolymers have been designed towards the goal of creating molecules that can penetrate membranes at endosomal pH to deliver their ODN cargo into the cytoplasm. The characterization of the polymers by the pyrene and hemolysis assays provides some insight regarding how the grafting chemistry influences these key properties of PPAA. The results from these assays indicate that the parent polymer, PPAA, undergoes a pH-dependent conformational change that imparts significantly greater hydrophobicity at pH 5.0 to 5.5 as compared to pH 6.0 and above. The hemolytic activity likewise exhibits a maximum at acidic pH, that of endosomes. This physical property of PPAA suggests that the incorporation of this polymer into DOTAP/ODN complexes can mediate timely destabilization of endosomes and release of the contents into the cytoplasm, thereby allowing the antisense ODN to bind with complementary mRNA. Previous fluorescence microscopy

has indicated that addition of PPAA to DOTAP/ODN complexes allows for the release of ODNs from endosomes, and that doing so results in an enhanced antisense effect [74].

In the case of the graft copolymers, we did not observe any significant red blood cell hemolysis throughout the pH range of 5.0–7.0, suggesting that the intracellular mechanism that these polymers employ to initiate carrier escape from endosomes is different from that of PPAA. Interestingly, the pyrene assay demonstrated that the graft copolymers, PPAA-g-PEO and PPAA-g-Jeffamine, displayed significant degrees of hydrophobicity over the entire pH range of 5.0 to 7.0, suggesting favorable interactions with the hydrophobic membranes of the cell and endosome. These results suggest that the graft copolymers behave differently in terms of their association with the cell and intracellular membranes. It is likely that the pH-insensitive hydrophobic components of the graft copolymers facilitate entry into cells and escape from endosomes by a fusion-mediated process as opposed to the pH-dependent lysis effects mediated by PPAA. Similar interactions with cell membranes were found with Pluronics, triblock copolymers of PEO-b-PPO-b-PEO architecture [46]. Previous work by Kabanov et al. demonstrated successful drug and gene delivery with Pluronic-PEI conjugates [37]. The efficacy of the Pluronics has been attributed to 1) favorable interactions between propylene oxide blocks of the polymer and the cell lipid bilayer membranes, leading to enhanced translocation into cells and 2) the formation of micelles that aid in the release of block copolymers into the cell [2, 37]. However, the organization of hydrophobic groups on the polymer also seems to play a role. While PPAA-g-PEO possesses hydrophobic domains from the PPAA backbone that can bind a small dye such as pyrene, the highly grafted PEO chains inhibit interactions of the PPAA-g-PEO copolymer with cells.

Thus, the PPAA-g-Jeffamine graft copolymer has been developed as part of a formulation designed to satisfy the following important prerequisites for cellular ODN delivery in biological milieu: (1) serum-stability, (2) uptake of ODNs into cells, and (3) release of ODNs into the cytoplasm before lysosomal degradation. The DOTAP/PPAA-g-Jeffamine formulation is also effective for delivery of siRNA (Peddada et al., unpublished data), thus proving to have broad application in technologies for gene silencing. While PPAA is effective at mediating intracellular delivery, it inhibits cellular uptake in the presence of serum. While PPAA-g-PEO may resist the attack of serum, this polymer appears to resist cellular uptake. On the other hand, PPAA-g-Jeffamine appears to strike an appropriate balance of hydrophilic/lipophilic character to allow serum resistance, cellular uptake, and endosomal escape. This graft copolymer can be tuned to further improve delivery or tailor the delivery system for a particular application. Thus, the PPAA-g-Jeffamine copolymers hold substantial promise as excipients for oligonucleotide delivery.

CHAPTER 3: EFFECT OF HYDROPHILIC-LIPOPHILIC BALANCE ON ANTISENSE GENE DELIVERY AND IN VITRO GENE SILENCING EFFECT

3.1 ABSTRACT

In our previous work, we designed a polymer-containing carrier system with dual functionalities, achieving both membrane lysis at acidic pH, and serum-stability. We found that altering the properties of the parent polymer, PPAA, has significantly altered the key functionality of PPAA that is its membrane lysis property at acidic pH. Here, we design a range of graft copolymers with varying degrees of hydrophilicity to hydrophobicity ratio, which we term hydrophilic factor 'HF'. We examine the effect of 'HF' on gene delivery processes by performing mechanistic studies involving evaluation of serum-stability, membrane penetration activity and membrane lysis at acidic and neutral pH. Furthermore, we deliver antisense oligonucleotides targeting bcl-2, which is over-expressed in A2780 ovarian cancer cells, and evaluate the efficiency of each of the graft copolymers with varying degrees of HF. We find that HF affects all the major steps in the delivery of antisense, correlating strongly with membrane penetration and in vitro gene silencing in 10% serum-conditions. These structure-function relationships help to design guidelines for improved antisense carrier chemistries.

3.2. INTRODUCTION

Polymer systems have been explored extensively as a means to overcome gene delivery barriers [31, 85]. Of interest in this work has been to target two key gene delivery barriers, one extra- and one intracellular. The extracellular barrier of carrier instability in the presence of serum greatly hinders delivery before the cargo reaches the

cell surface. The intracellular barrier of endolysomal degradation degrades the carrier by releasing enzymes in the acidic environment. Several research groups have employed the approach of combining two polymer chemistries, each to overcome a key barrier. In this work, we employ this approach. PPAA, (poly propyl acrylic acid), a member of the acrylic acid family of polymers, possesses the unique property of displaying pH-sensitive membrane lysis with lysis at acidic or endosome pH, and absence of lysis at neutral or cytoplasmic pH. The incorporation of PPAA with DOTAP/ODN complexes provides success in non-serum media, however fails in the presence of serum media. Therefore, the approach here has been to create graft copolymers with hydrophobicity and varying hydrophilicity by conjugating PPAA, a hydrophobic polymer, and poly (alkylene oxide) polymer, a hydrophilic polymer. We take our previous work a step forward by designing a panel of graft copolymers and assess their effects on the major steps in the gene delivery process. Finally, we draw conclusions that help us learn how the chemistry can be optimized for overall enhanced delivery and antisense gene silencing effect.

The potential for non-viral carriers can be improved by drawing relationships between chemistry of carriers and their effects on antisense delivery. Several groups have studied the effects of physicochemical variables -- including nanoparticle size, surface charge, hydrophilicity/hydrophobicity, presence of pH buffering/lysis groups on polymer, polymer molecular weight -- on nucleic acid and delivery [45, 86]. The chemistry of carriers has been tailored to overcome gene delivery barriers. It has been found that size and shape of the nanoparticle impacts the biodistribution of the nanoparticle once in the bloodstream, that is whether accumulation in the kidney, RES (liver, spleen) or tumor by the passive EPR effect takes place [52, 87]. At the cellular level particle size has been

shown to dictate the method of endocytosis entry into cells [88]. The importance of hydrophilicity is represented by incorporating PEG to coat and stabilize nanoparticles [89], while recognizing that at the cellular level, particles must also be hydrophobic for cellular entry. We focus on studying the effects of polymer hydrophilicity/hydrophobicty on cellular uptake, pH-sensitive lysis for endosome escape and overall antisense delivery. The size and particle surface charge of the nanoparticles are fairly similar, allowing us to isolate and understand the effect of 'HF' (hydrophilic factor) on antisense gene delivery.

3.3 MATERIALS AND METHODS

3.3.1 Synthesis of graft copolymers

The synthesis of graft copolymers is described for the 10% grafting of Jeffamine M2070 onto PPAA and is similar for Jeffamine M-2005 and PEO graft chemistry (Scheme 1).

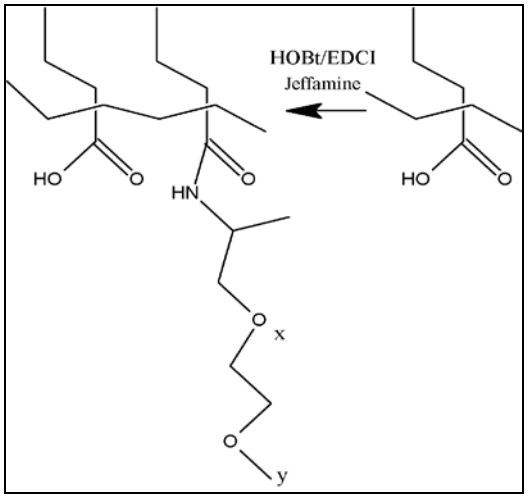

Scheme 2: Reaction scheme for synthesis of graft copolymers (image represents Jeffamine grafting)

For 10% grafting of Jeffamine M2070, molecular weight 2000Da: Poly (propylacrylic acid) (50 mg, 0.44 mol of repeat units) was taken in a dry 10 mL round bottomed flask. HOBt (9 mg, 0.044 mmol) and diisopropylcarbodiimide, DIPC(10.2 uL, 0.044 mmol) were added to the flask. Dry THF (5 mL) was added to the flask and the reaction was stirred at room temperature for 45 min. After this, amine-terminated Jeffamine M-2070 (88 mg, 0.044 mg) was added and the reaction was stirred at 50^{O}C for 30h. After the reaction time, THF was removed and samples were dried and resuspended in a solution of 10% by volume 1N NaOH and 90% PBS pH 7.4. This mixture was transferred to a Pierce Dialyzer cassette (MWCO 10000) and dialyzed against dH2O for 2 days with buffer changes every 2 hrs for the first 6 hrs and every 4-6 hrs thereon. After the 2 days, product was then removed, lyophilized and then characterized by NMR. There are three methods to calculate graft density by using CH3 group of PPAA and: 1) amide peak of the conjugate at 7.8 ppm, 2) CH3 peak of Jeffamine (propylene oxide), where one CH3 of PPAA corresponds to 10 CH3 of Jeffamine (propylene oxide) to denote 100% grafting, and 3) CH2 peak of ethylene oxide and propylene oxide, where 3H of PPAA will correspond to 144H of Jeffamine/mol for 100% grafting. The amide peak, although most accurate in determining the degree of conjugation, is a very small peak to integrate, hence proving to be inaccurate. Therefore, methods 2 and 3 were used to determine degree of grafting density of Jeffamine and PEO, respectively, onto PPAA.

3.3.2 Cell culture

A2780 (ovarian cancer cells) were obtained from American Type Culture Collection. Cells were maintained in RPMI 1640 medium supplemented with 10% fetal bovine serum, 100 U/ml penicillin, and 100 ug/ml streptomycin.

3.3.3 Nanoparticle Preparation

Complexes were prepared using a DOTAP/ODN weight ratio of 10:1, which corresponded to a charge ratio of 4.7 (+/-) and a DOTAP/ODN/polymer charge ratio of 1.0. The net charge ratio is defined as the ratio of the moles of DOTAP amine groups to the sum of the moles of ODN phosphate groups and PPAA carboxylic acid groups.

3.3.4 Particle sizes

Particle sizes of complexes were measured in PBS and 10% serum-containing media to determine the stability of complexes and the effect of grafting hydrophilic moieties onto PPAA. Particle sizes were measured at the optimum charge ratios of DOTAP/ODN, 4.7, and DOTAP/ODN/Polymer, 1.0, as determined by previous work [90].

3.3.5 Hemolysis effect

The ability of PPAA and the grafted polymers to disrupt membranes was assessed using a hemolysis assay. Solutions of PPAA and graft copolymers were added to pH buffers 5.0, 5.5, 6.0, 6.5 and 7.0 at equivalent moles of carboxylic acid groups and vortexed thoroughly. To these polymer solutions, fresh RBCs that had been washed three times with 100 mM NaCl were added at a concentration of 10^8cells/ml, incubated in a waterbath at 37^oC for 1 hr, and then centrifuged for 4 min at 400 *g* to pellet the intact RBCs. The absorbance of the supernatant was measured at 541 nm using UV spectrophotometer. Experimental controls included RBCs in pH buffers in the absence of polymer (negative control) and RBCs in distilled water (positive control). Red blood cells were used within two days of isolation.

$$\%\ HEMOLYSIS = \frac{(Abs - Abs\ o)}{(Abs\ max.)} * 100,$$

$$Abs = Abs.\ polymer\ in\ pH\ buffer\ with\ RBCs, Abs\ o = Abs.\ pH\ buffer\ with\ RBCs$$

$$Abs\ max. = Abs.\ RBC\ in\ Triton\ X - 100$$

3.3.6 Calcein dye leakage from DPPC liposomes

DPPC liposomes were prepared following the general protocol provided by Avanti Polar Lipids with alteration in the procedure to include loading of a dye. Briefly, the first step involved obtaining a thin lipid film, followed by hydration of the lipid film with calcein dye by agitation and heat/stir at 50C for 2 hrs (this temperature is greater than the phase temperature of the lipid). The weight ratio of DPPC lipid to calcein was 1:3. The samples was agitated and sonicated for 15 mins to form lamellar vesicles, following by 5 cycles of freeze/thaw and extrusion using a 100nm polycarbonate membrane. Finally, unloaded calcein dye was separated from DPPC liposomes using a Sephadex column. For the membrane penetration assay, PPAA and graft copolymers at various concentrations were incubated with calcein loaded DPPC liposomes for 1 hr at 37°C in pH buffer solution of 7.4, followed by measuring release of calcein fluorescence relative to control. Incubation of dye-loaded DPPC liposomes with Triton X-100 was regarded as 100% calcein release. Calcein fluorescence is measured at excitation of 490 nm and emission of 520 nm. The equation is as follows:

$$\%\ CALCEIN\ LEAKAGE = \frac{(F - Fo)}{(Fmax - Fo)} * 100,$$

$$Fo = fluor.liposomes\ without\ calcein, F = fluor.liposomes\ with\ calcein\ and\ polymer,$$

$$Fmax. = Fluor.liposomes\ with\ calcein\ and\ Triton\ X - 100$$

3.3.7 Serum-stability

The stability of complexes in the presence of serum was evaluated by exposing complexes to 50% serum (FBS) for 1 hr at 37C, followed by inactivation of serum at 70°C for 10 mins. Antisense ODN was visualized by staining agarose gel with Sybr green dye. Complexes were prepared in the presence and absence of serum and percentage of intact ODN was calculated relative to untreated (no serum) for that particular condition. As a control, naked ODN was used which shows maximum degradation in the presence of serum. A agarose gel of 1.5 % was used and conditions for running the gel were 70V for 40 mins, and staining of the gel was performed in 1:10000 Sybr green in TE buffer for 45 mins in the dark.

3.3.8 In vitro gene silencing

Quantitative measurements of Bcl-2 gene silencing were obtained using real-time PCR at 24 hours post-treatment. The bcl-2 antisense sequence, G3139, follows the sequence 5′-TCTCCCAGCGTGCGCCAT-3′. Cells were seeded onto 12-well plates at 10^5cells/ml (with 1 ml volume per well) ~18 h prior to ODN treatment. The final concentration of ODN used for in vitro gene silencing experiments was 300 nM. In the case of treatment, 200 µl of complexes were prepared, mixed with 10% FBS-containing medium and added to each well. For control samples, complexes were substituted with 200 µl of PBS. After 4 hours of cell exposure to treatment, medium containing complexes was aspirated and replaced by fresh medium. Cells were assayed for bcl-2 gene expression 24 hrs post-ODN treatment using real-time PCR. The ΔΔCt method was used to calculate % Bcl-2 gene expression.

$$\%\ Bcl2\ gene\ expression = 2^{-1(\Delta\Delta Ct)} * 100, \Delta\Delta Ct = \Delta Ct(treatment) - \Delta Ct(control),$$

$$\Delta Ct = Ct(bcl2) - Ct(18S)$$

3.3.9 In vitro cell metabolic activity

Cells were cultured on 96-well plates and treated with the various graft copolymer formulations as described in the previous section 'NP Preparations'. Following this, cells were assayed for cell metabolic activity using the MTS assay at various time points (48, 72 and 96 hrs post-treatment) by measuring absorbance of product at 260 nm.

$$\%\ CELL\ METABOLIC\ ACTIVITY = \frac{Abs\ (treatment)}{Abs\ control\ (untreated\ cells)} * 100$$

3.3.10 Statistics

All statistical analyses were performed by a one-way ANOVA test and results were represented as mean ± standard deviation. Pair-wise comparisons between the various polymer-containing delivery systems were made using the Tukey HSD post-hoc test; a p-value less than 0.05 indicated significant differences compared with control, as indicated by asterisks on figure plots.

3.4 RESULTS

3.4.1. Synthesis and characterization of graft copolymers

The degree of graft density was calculated using NMR peaks from the graft polymer relative to the propyl groups of PPAA. For the 10% PEO graft copolymer, the grafting reaction was confirmed using the amide peak of the conjugate relative to propyl peaks of PPAA, however since a large amount of material is required to visualize the amide peak and inaccuracies exist in integrating this relatively small peak, we resorted to using other peaks from the graft copolymer to determine the degree of graft density (See

Methods section). The unreacted graft polymer was removed by dialysis. The dialysis step was extended by 2-3 days to ensure that all unreacted graft polymer was removed.

Below is a table of the various graft copolymers synthesized and their NMR graft density, solubility and HF. We define the term HF to represent the degree of polymer hydrophilicity.

Graft polymer/ Molecular Weight	Graft copolymer	Target graft density (mol %)	NMR graft density (mol%)	Solubility	HF* (value for PPAA is 0)
Jeffamine M-2070/2kDa	'Pg1%J70'	1	3	Aqueous	0.07
Jeffamine M-2070/2kDa	'Pg5%J70'	5	8	Aqueous	0.19
Jeffamine M-2070/2kDa	'Pg10%J70'	10	11	Aqueous	0.26
Jeffamine M-2005/2kDa	'Pg1%J05'	1	2	Aqueous	-0.02
Jeffamine M-2005/2kDa	--	5	-	Organic	-0.06
PEO/2kDa	'Pg1%PEO'	1	3	Aqueous	0.13
PEO/2kDa	'Pg5%PEO'	5	12	Aqueous	0.52
PEO/2kDa	'Pg10%PEO'	10	23	Aqueous	1.00

Table 3.1: Panel of graft copolymers with percentage graft density (target and NMR), solubility characteristics and hydrophilic factor (HF). Note molecular weight of parent polymer, poly (propyl acrylic) acid, is 200 kDa.

$$HF: \frac{\text{H(graft copolymer)-H(PPAA)}}{\text{H(max.)}},$$

$$H(graft\ copolymer) = \sum (n(COOH) * Group\ no.1) + (n(EO) * Group\ no.2) + (n(PO) * Group\ no.3),$$

$$H(PPAA) = \sum (n(COOH) * Group\ no.1)$$

HF=Hydrophilic Factor, H=hydrophilicity, n=number of moles, EO=ethylene oxide, PO=propylene oxide, H (max.)= hydrophilicity of PPAA-g-10%PEO, Group no. 1=2.1, group no. 2=0.35, group no.3=-0.125 (values from group nos. taken from "Colloids and interfaces with surfactants and polymers: an introduction" [91])

3.4.2 Particle Sizes

DOTAP/ODN lipoplexes exhibited a mean size of approx. 400 nm, and the addition of PPAA to these lipoplexes increased the size slightly too approx. 480 nm (Figure 3.1). The addition of graft copolymers to the DOTAP/ODN complexes induced a reduction in the particle size. Addition of PPAA-g-1%Jeffamine M 2070 and PPAA-g-1%PEO to DOTAP/ODN reduced the particle size to ~300 nm.

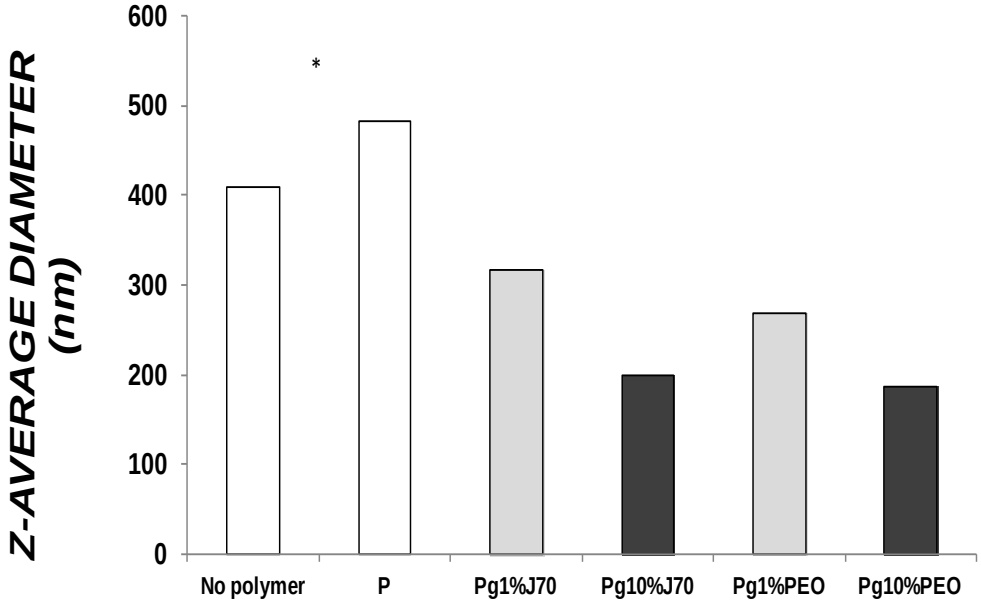

Figure 3.1: Particle sizes of DOTAP/ODN 'No polymer', DOTAP/ODN/PPAA 'P', followed by graft copolymer as indicated. The charge ratio of DOTAP/ODN is 4.7 and DOTAP/ODN/Polymer is 1.0. Measurements were taken 30 minutes following complex preparation (3 runs, 3 mins/run). DOTAP/ODN indicated as 'No polymer', PPAA 'P', PPAA-g-1%Jeffamine 2070 'Pg1%J70', PPAA-g-10%Jeffamine 2070 'Pg10%J70', PPAA-g-1%PEO 'Pg1%PEO' and PPAA-g-10%PEO 'Pg10%PEO'. p value <0.05, error bars represent standard deviation.

3.4.3 Hemolysis effect of PPAA and PPAA graft copolymers

A critical step in the process of antisense delivery is the escape of the carrier from endolysosomal degradation, a major intracellular barrier for the successful delivery of ODN to the target site of action. The approach in this work involved the use of a pH-sensitive lytic polymer, poly (propyl acrylic acid) or 'PPAA'. Previous work showed that higher grafting density of polymer onto PPAA (10 mol%) diminished hemolysis effect, however still retained gene delivery and silencing effect [90]. This result demonstrated that endosome lysis as mediated by PPAA is most likely not the mechanism of endosome escape employed by this graft copolymer complex, but instead an alternate mechanism such as membrane fusion.

We evaluated the ability of the graft copolymers to exhibit pH-dependent hemolysis, which has been associated with the ability to escape the endolysosomal pathway within cells [36]. Grafting of hydrophilic polymers onto PPAA alters the ionization at acidic pH, thus affecting the overall polymer conformation which is believed to dictate the degree of membrane lysis. The data shows that at the pH of 6.0, that of the endosomes, the 1mol% PEO grafting retains most of the membrane lysis effect of the parent polymer, PPAA, while the 1mol% grafting of Jeffamine M 2070 reduces lysis effect (Fig.3.2). Grafting densities of 5 and 10 mol% eliminate the lysis effect (hence not shown on graph). At the pH of 6.0, PPAA displays maximum lysis effect followed by PPAA-g-1%PEO, while PPAA-g-1%Jeffamine M 2070 and PPAA-g-1%Jeffamine M 2005 display negligible lysis. The polymers PPAA, PPAA-g-1%PEO and PPAA-g-1%Jeffamine M 2070 do not display lysis at neutral pH of 7.0, while the 1%Jeffamine M 2005 displays maximum lysis at pH 7.0.

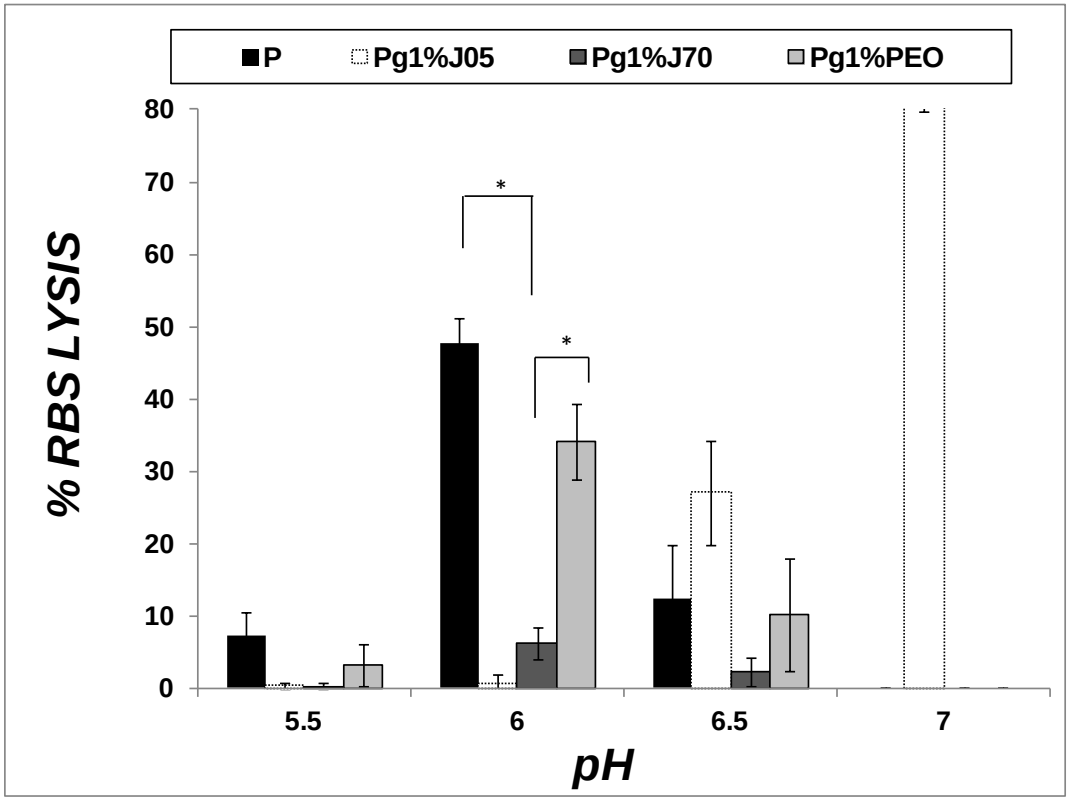

Figure 3.2: Hemolysis effect by PPAA and graft copolymers (PPAA MW=200 kDa). Grafting of poly (alkylene oxides) onto PPAA reduces hemolytic activity of PPAA 'P'. The extent of hemolysis was calculated using control, RBC in various pH buffer solutions, and normalized to 100% lysis induced by cells in distilled water. Nomenclature of polymer as indicated in Figure 3.1 and Figure 3.2 (n=3, errors bars represent sd, for significance p value <0.05)

3.4.4 Degree of membrane penetration

The release of calcein dye from dye-loaded liposomes is indicative of the degree of membrane penetration of the polymers through liposome membranes that occurs either by fusion or lysis. This assay provides insight to understanding how the chemistry of poly (alkylene oxide) or PAO, PEO/Jeffamine M2070, and degree of grafting density of PAO onto PPAA affects the ability of the polymer to associate with and disrupt liposome

membranes at neutral pH. The differences between graft copolymers to induce calcein dye leakage are apparent at 6.3 and $10.3*10^{-9}$ COOH groups/ug polymer (Fig 3.3). PPAA displays the greatest calcein release throughout the range of polymer concentrations, followed by decreasing calcein release with increasing graft densities of PAO onto PPAA. The 1% grafts of PEO (HF=0.13) and Jeffamine M 2070 (HF=0.07) demonstrate fairly similar extents of calcein release, while at 5 mol%, and even more pronounced at 10 mol%, the differences between the two chemistries become apparent (Fig 3.3). At the concentration of 6.3 COOH gps/polymer (*10^-9), the 5mol% Jeffamine M 2070 grafted polymer with HF of 0.19 displays greater calcein release (~35%) compared to 5% mol% PEO with HF of 0.52 and calcein release of 20%. The difference in calcein release between Jeffamine (HF=0.26) and PEO (HF=1.00) is greater at the 10 mol% grafting, with 25% and 0%, respectively. These results indicate that at higher grafting densities the membrane penetration of Jeffamine M 2070 is greater than that of PEO, highlighting the importance of hydrophobic PO groups of Jeffamine compared to solely EO groups of PEO.

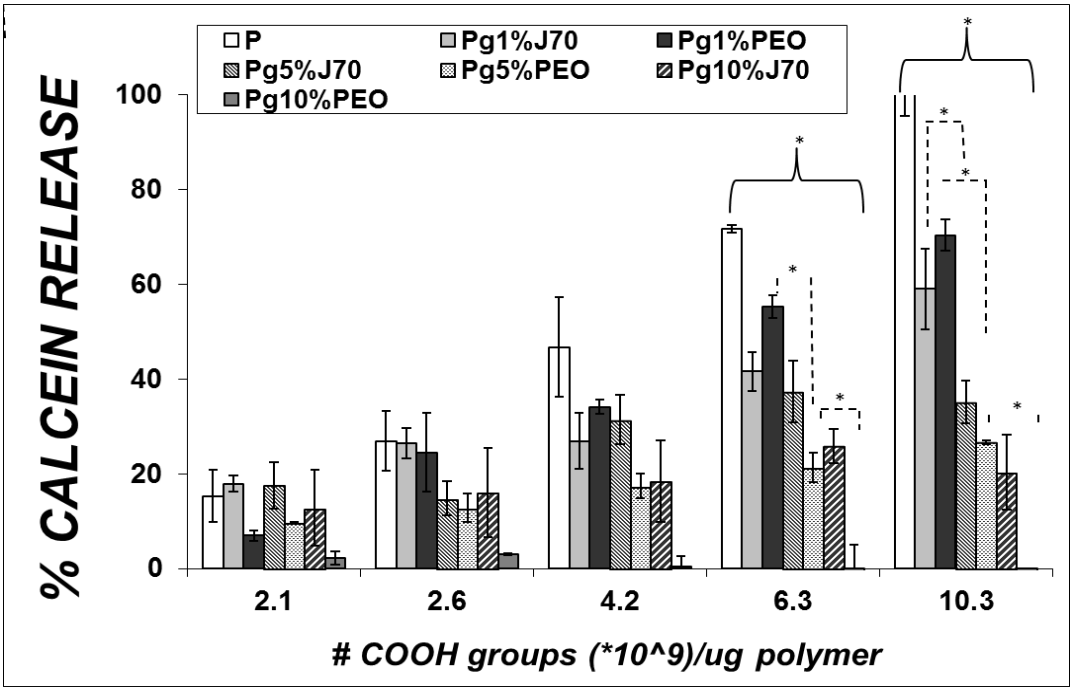

Figure 3.3: Calcein release from DPPC liposomes incubated with PPAA and graft copolymers. Polymer nomenclature is as indicated in Figures 3.1 and 3.2. The control of 100% calcein release was obtained by incubation of DPPC liposomes in triton X-100 surfactant, and calcein dye was measured by excitation/emission of 480/530 nm. (n=3, errors bars represent sd, significance p value <0.05).

3.4.5 Serum-stability of complexes

Figure 3.4 shows an agarose gel with complexes of DOTAP/ODN with PPAA, PPAA-g-1%Jeffamine (M 2070) and PPAA-g-1% PEO, where antisense ODN alone is used as control to represent maximum degradation. This image clearly demonstrate that addition of 1% grafting of Jeffamine M-2070 or PEO enhances serum stability, compared to PPAA, in the presence of FBS, as indicated by greater percentage of antisense ODN retained in the intact band and lesser ODN in the degraded portion (as indicated by the smear).

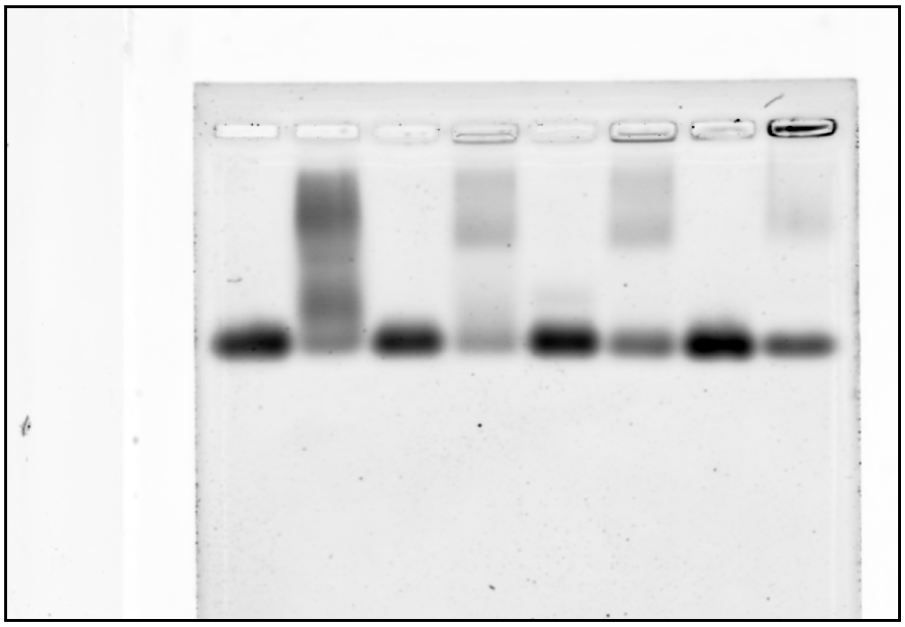

Figure 3.4: Serum-stability of polymer-containing DOTAP/ODN complexes. Image of agarose gel stained with Sybr green to detect ODN in intact and degraded forms. Complexes were prepared as described in the methods. The charge ratio of DOTAP/ODN is 4.7 and with polymer 1.0. Samples are indicated as ODN, ODN+FBS, DOTAP/ODN/PPAA 'PPAA', DOTAP/ODN/PPAA+FBS ('PPAA+FBS'), and so on.

3.4.6 Bcl-2 gene silencing in A2780 ovarian cancer cells

The ability of graft copolymer complexes to deliver ODN and silence bcl-2 target gene in A2780 ovarian carcinoma cells was evaluated using quantitative PCR. The expression of bcl-2 was evaluated 24 hrs post-treatment, where ODN silencing effects are maximum. The complex of DOTAP/ODN showed 80% bcl-2 gene expression compared to control, untreated cells with 100% bcl-2 gene expression (Fig.3.5A). The addition of PPAA to DOTAP/ODN complexes improved antisense gene delivery and silencing effects, reducing bcl-2 gene expression to 40%. This enhanced silencing effect by the addition of PPAA is similar to that observed in previous work using CHO-d1EGFP cells

[90]. The addition of 1% Jeffamine and PEO grafted polymers further improved antisense gene silencing compared to PPAA, with bcl-2 gene expression levels of 10 and 15%, respectively (Fig. 3.5A). However, addition of 5 and 10 mol% grafted Jeffamine and PEO polymers progressively decreased gene silencing as seen with increasing bcl-2 gene expression levels. For 10 mol% graft densities, gene silencing levels were higher for Jeffamine grafted polymer compared to PEO grafted polymers. For the conditions treated with scrambled antisense, bcl-2 gene expression levels were in the range of 60-80% (Fig 3.5B). These levels of expression are not surprising for antisense, which is known to have non-specific gene silencing effects. This result is similar to that observed in previous work with GFP antisense to treat CHO-d1EGFP cells [90].

(A)

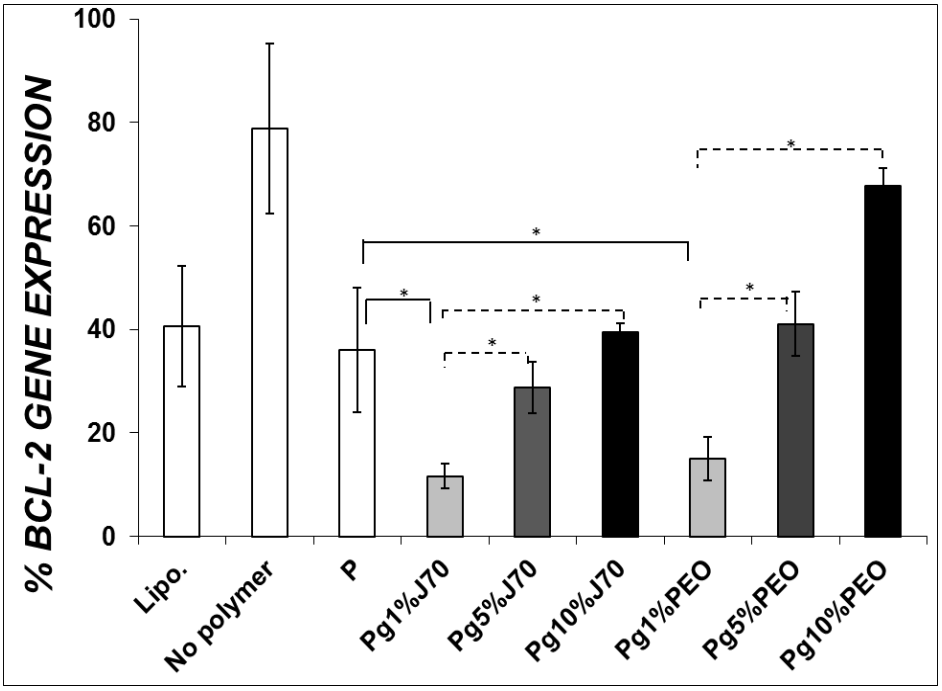

Figure 3.5: Bcl-2 gene silencing in A2780 cells upon treatment with various complexes containing (A) sequence-specific for 4 hrs under 10% FBS-containing media conditions. Bcl-2 gene levels were measured 24 hrs from the start of treatment. The net charge ratio for DOTAP/ODN ('No polymer') was 4.7 and DOTAP/ODN with various polymers was 1. PPAA is 'P', PPAA-g-1%Jeffamine M2070 is 'Pg1%J70' and so on. ODN concentration was 300 nM, gene expression was measured relative to untreated cells. (n=3, errors bars represent sd, significance p value <0.05)

(B)

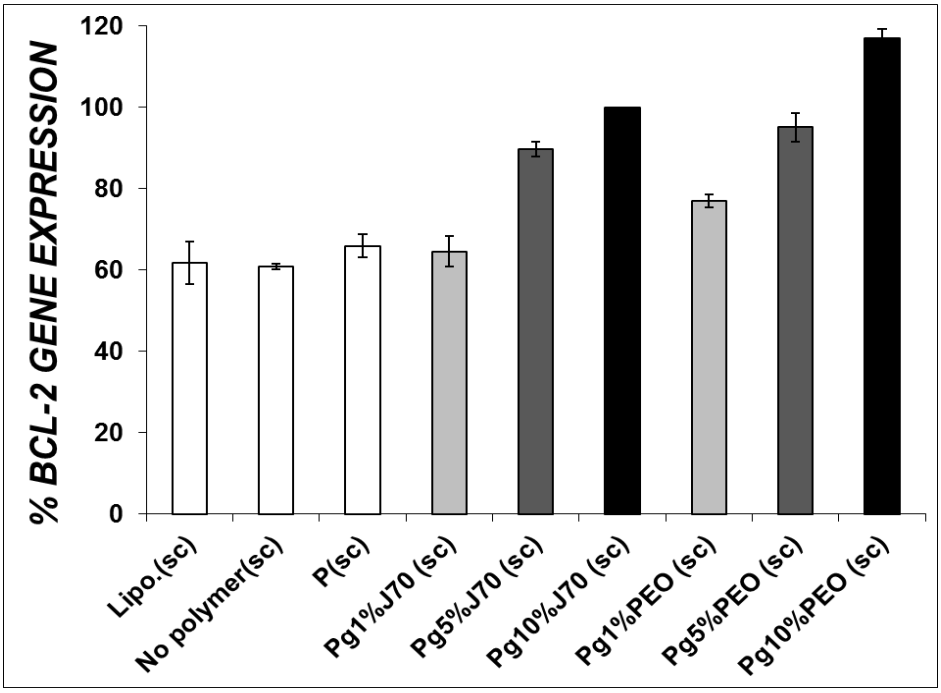

Figure 3.5: Bcl-2 gene silencing in A2780 cells upon treatment with various complexes containing (B) scrambled Bcl-2 ODN for 4 hrs under 10% FBS-containing media conditions. Bcl-2 gene levels were measured 24 hrs from the start of treatment. The net charge ratio for complexes and carrier nomenclatures is the same as indicated in Figure 3.5A (with 'sc' indicating scrambled).

Cellular metabolic activity was evaluated upon treatment of carriers with antisense bcl-2 were to determine (1) whether bcl-2 gene silencing is sufficient to alter cell metabolic activity, and (2) whether the carrier demonstrates cytotoxicity at these concentrations. The effect of carriers on cell metabolic activity is similar when sequence-specific and scrambled sequences are used, proving that the cytotoxic effect is unrelated to a gene silencing effect but instead related to carrier cytotoxicity. This data indicates

that the most hydrophobic polymer, PPAA-g-1%Jeffamine M 2005 (‘Pg1%J05’), is significantly more cytotoxic compared to all the other carriers (except PPAA) (Fig. 3.6). The cytotoxicity induced by the carrier is directly related to carrier hydophobicity and this reduces with decreasing hydrophobicity, as can be seen with increasing graft density (indicating increasing degree of hydrophilicity).

(A)

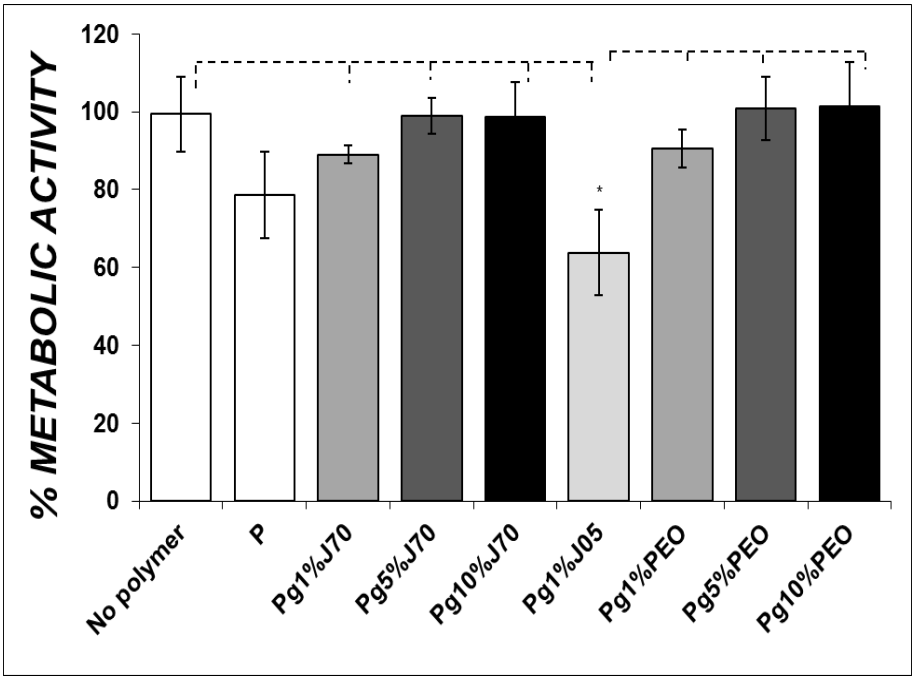

Figure 3.6: A2780 cell metabolic activity upon treatment with various complexes containing (A) sequence-specific for 4 hrs under 10% FBS-containing media conditions. Cell metabolic activity was measured 48 hrs from the start of treatment using the MTT assay. The net charge ratio for complexes and carrier nomenclatures is the same as indicated in Figure 3.5A. (n=3, errors bars represent sd, significance p value <0.05)

(B)

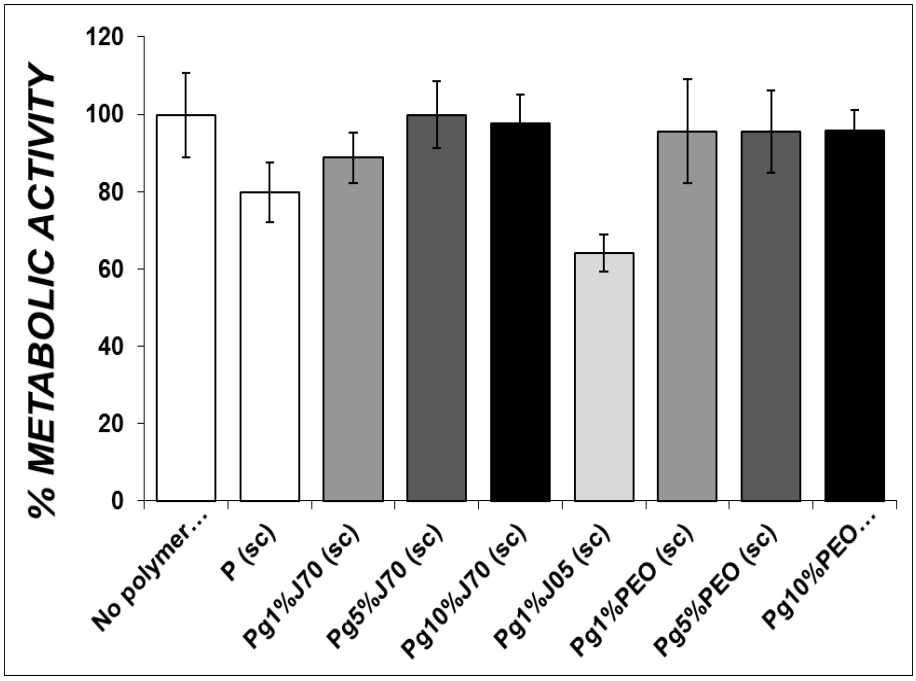

Figure 3.6: A2780 cell metabolic activity upon treatment with various complexes containing (B) scrambled sequence for 4 hrs under 10% FBS-containing media conditions. Cell metabolic activity was measured 48 hrs from the start of treatment using the MTT assay. The net charge ratio for complexes and carrier nomenclatures is the same as indicated in Figure 3.5B.

3.5 DISCUSSION

We have developed a self-assembled nanoparticle designed to achieve multiple functions of extracellular serum-stability and for cellular entry and intracellular endosomal escape. Here, in this chapter we focus on studying the effects of the hydrophilic factor, HF, on various steps of the gene delivery process, specifically serum-stability, membrane penetration (cellular entry), and pH-sensitive membrane lysis (endosome escape), and determine finally how all these affect antisense gene silencing. This section contributes to the understanding of structure-function, thereby provides useful guidelines for designing improved antisense ODN carriers.

Previous work has characterized the carrier system, DOTAP/ODN/PPAA, for delivery in non-serum and serum-containing media and determined lower antisense delivery efficiencies in the presence of serum, therefore posing the need for an improvement by modifying the DOTAP liposome or PPAA polymer chemistry. In this study, the PPAA chemistry has been modified with hydrophilic poly(alkylene oxide) polymers to create a panel of graft copolymers with varying HF (hydrophilic factor) as determined by graft chemistry, PEO or Jeffamine of ethylene oxide/propylene oxide of 31/10, and grafting density. The benefit of utilizing copolymers with multiple functionalities serves the purpose of incorporating one polymer into the delivery system, thereby reducing the number of components of the nanoparticle. Several groups have adopted this approach by creating graft or block copolymers. Some examples in the area of polycations include, PEI-g-PEG and PEI-g-Pluronic, and in the area of liposomes include PEG-lipids [68, 69, 92]. The balance of achieving the benefits of both units, without hampering one function or the other, is essential.

Our results indicate that 1mol% graft density of polymer onto PPAA is most effective, after which any increase in graft density to 5 and 10 mol% decreases serum-stability, membrane penetration, hemolytic effect, and overall in vitro gene silencing effect. A relatively simple metric of the copolymer hydrophilicity, HF, appears to be related to each of these assay outputs, which in turn are widely accepted as indicators for key steps in nucleic acid delivery. The relationship between Bcl-2 gene expression (upon treatment with antisense) and HF shows that at HF values of 0.07 and 0.13, the Bcl-2 gene expression is lowest (indicating maximum antisense gene silencing), and as HF increases, the Bcl-2 gene expression levels progressively increase, with levels of expression the same as or higher than PPAA. In the case of membrane penetration as a function of HF, the data indicates that PPAA, the most hydrophobic (HF=0), displays maximum membrane penetration, after which the degree of membrane penetration (indicated by release of calcein dye from liposomes) decreases with increasing HF (Fig.3.6). Further, PPAA displays maximum membrane lysis at pH 6.0 (acidic pH that of endosomes), with no broad correlation with HF. Instead, the degree of membrane lysis seems to be an all or none effect with no gradual decrease in lysis as a function of grafting density. Our previous data indicated an elimination of membrane lysis at acidic pH upon grafting PPAA with hydrophilic polymers; however, the antisense oligonucleotide delivery was unaffected, indicating that there exists other mechanism of cell entry or endosome escape that is different from the action of PPAA. In regards to the impact of polymer grafting on serum-stability, the data indicates that upon incubation of carriers with 50% serum at 37C, 1 mol% grafting of both PEO and Jeffamine M 2070 retains intact ODN, while PPAA alone shows degradation of ODN due to a lack of

protection from hydrophilic groups. In Figure 3.7A we see that the calcein release correlates well with HF for all polymers, indicating that the association of polymers with membranes decreases with increasing hydrophilicity. PPAA, the most hydrophobic polymer, displays the highest association with membranes. The bcl-2 gene silencing data (Figure 3.7C), however, mostly correlates with HF, except for PPAA, the polymer with lowest HF, which does not show maximum gene silencing effect. In our previous work (Chapter II), we see that PPAA is most effective in serum-free conditions, and grafting with hydrophilic moieties reduces antisense gene delivery (in non-serum) as a result of lower association with cells. However, in the presence of serum, serum-stability is most important compared to the degree of membrane penetration, and therefore dictates the gene silencing effect. The gene silencing effect in the presence of serum is dictated by the balance of hydrophilicity to hydrophobicty, proving that this parameter is important to optimize.

(A)

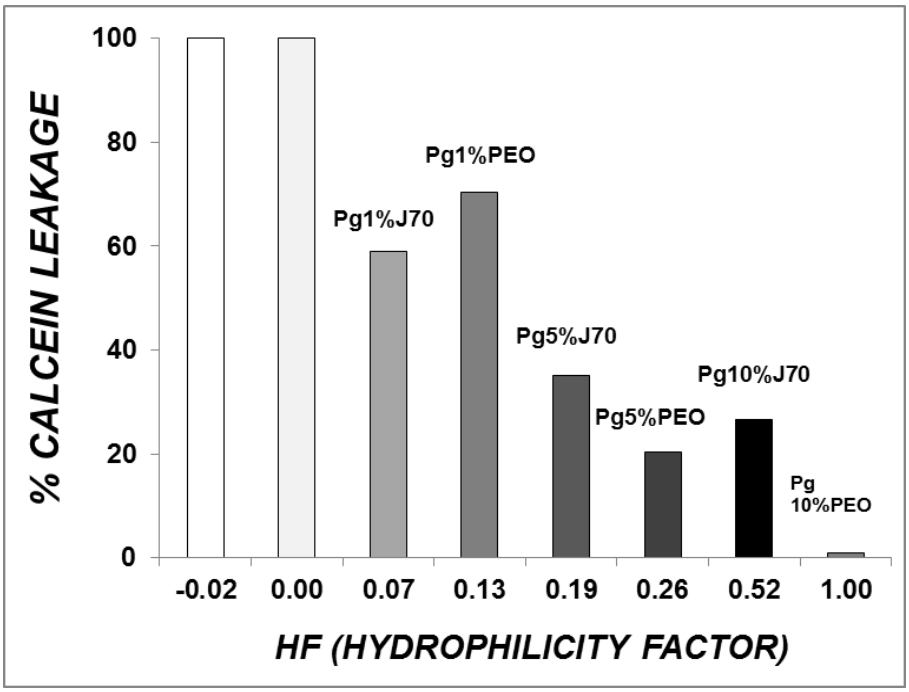

(B)

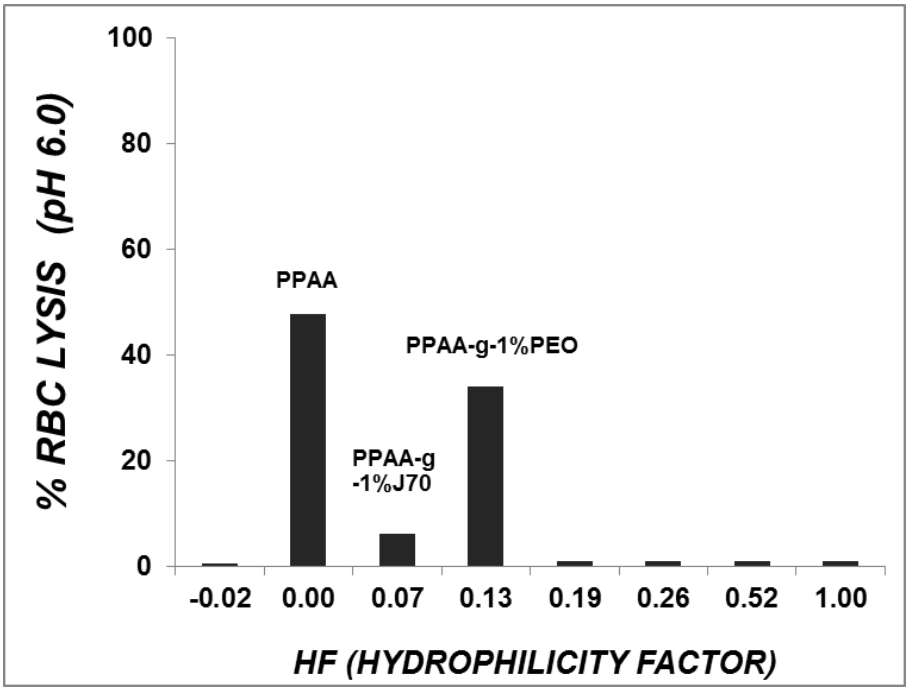

Figure 3.7: Effect of polymer HF on (A) Calcein dye release from DPPC liposomes, (B) RBC lysis at pH of 6.0

(C)

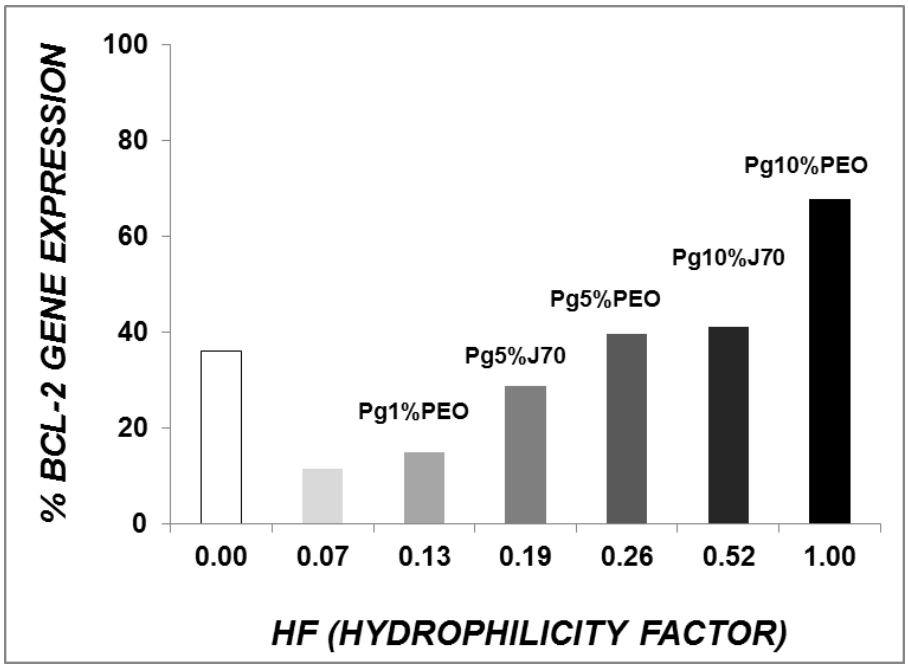

Figure 3.7: (C) % Bcl-2 gene expression upon delivery of bcl-2 antisense in DOTAP/polymer carrier systems. Polymers are as labeled above their respective bar.

CHAPTER 4: IN VIVO BIODISTRIBUTION PROFILES OF GRAFT COPOLYMERS (This work was performed in close collaboration with Dr. Tamara Minko, Dept. of Pharmacy)

4.1 ABSTRACT

Much research in the field of carrier development for nucleic acid delivery draws relationships between carrier chemistry and delivery efficiency based on in vitro results, but fails to validate the delivery system in vivo. This disconnect motivated the validation of the in vitro-characterized polymer delivery system to an in vivo tumor xenograft mouse model. We determine the biodistribution of 1 and 10 mol% PEO and Jeffamine-graft copolymers in comparison to the unprotected, DOTAP/ODN carrier system. The 1 mol% grafted copolymer shows significantly enhanced accumulation of Cy5.5 ODN in the tumor, as well as higher overall organ fluorescence, compared to 10 mol% grafting and unprotected carrier. This is consistent with our in vitro results, supporting both discovery -- utility of the 1 mol% grafted polymers – and analysis -- correlation among physicochemical assays, in vitro silencing and in vivo tumor distribution. Further, we determined the most effective degree of grafting to be 1 mol% since grafting higher (10 mol %) hinders delivery.

4.2 INTRODUCTION

We have designed a self-assembled nanoparticle that systemically delivers antisense oligonucleotides (ODNs) to a solid tumor more efficiently because of its hydrophilic nature, which has been associated with increased stability and half-life due to

reduced interaction with opsonins in the bloodstream [59, 71, 93]. Here, we study the biodistribution of these polymer-lipoplex complexes in vivo to understand the role of particle size and chemistry on distribution to the various organs, thus helping us understand how the reticuloendothelial (RES) system and EPR (enhanced permeation and retention) effect plays a role in affecting the fate of the antisense carrier. Previous work has developed and characterized this system for its increased serum-stability and antisense gene delivery, and here we hypothesize that these favorable properties will increase blood circulation time in vivo, resulting in greater accumulation at the tumor site. We hope to correlate our in vitro results with in vivo findings. In doing so, validating the design of the multi-functional nanoparticles and proposing improved chemistries.

Our approach was to employ a tumor xenograft model using the ovarian cancer cell line that was utilized in previous work. The A2780 cells were used because of their known property to form solid tumors in mice. The nanoparticles are injected intraperitonially to represent a systemic form of administration that allows the nanoparticle to enter and be degraded in the bloodstream, or accumulate in the RES organs of the liver and spleen, or in the kidney, lung or tumor. We assess the biodistribution profiles by tracking a fluorophore-labeled antisense oligonucleotide (ODN) that is targeted to the bcl-2 gene. At 24 hours post-i.p injection, the antisense will accumulate in the organs and if active in the tumor cells, elicit an antisense gene silencing response. The nanoparticle was formed by electrostatic interactions between the ODN and positively-charged liposome, DOTAP, followed by the complex of DOTAP/ODN and negatively-charged conjugates of pH-sensitive polymer, poly (propyl acrylic) acid (PPAA), and a poly (alkylene oxide) (PAO) polymer.

4.3 MATERIALS AND METHODS

4.3.1 Cell line

A2780 (ovarian cancer cells) were obtained from American Type culture Collection. Cells were maintained in RPMI 1640 medium supplemented with 10% fetal bovine serum, 100 U/ml penicillin, and 100 μg/ml streptomycin.

4.3.2 Preparation of complexes

Complexes of DOTAP/ODN in the presence of PPAA or PPAA graft copolymers were formed by electrostatic interactions, first between the cationic DOTAP liposomes and anionic ODN, and then between the DOTAP/ODN complexes and the anionic polyelectrolytes (PPAA and graft copolymers). Complexes were prepared using a DOTAP/ODN weight ratio of 10:1, which corresponded to a charge ratio of 4.7 (+/-) and a DOTAP/ODN/polymer net charge ratio of 1.0. The net charge ratio is defined as the ratio of the moles of DOTAP amine groups to the sum of the moles of ODN phosphate groups and PPAA carboxylic acid groups. The ODN is Cy5.5 labeled and sequence-specific to the bcl-2 gene.

4.3.3 Treatment of animals (Protocol closely follows work by Pakunlu et al.)

A2780 human ovarian cancer cells (~8 x 10^6) used for *in vitro* bcl-2 gene silencing were subcutaneously transplanted into the flanks of athymic mice (6-8 weeks old, ~20 g weight/mouse). Cells were collected at the same passage number over the course of the in vivo experiments. Cells were passaged at 70% cell density, the peak growth phase for cells. A2780 have been shown to form solid tumors in mice [94]. Once the tumor size reached a size of 200-800 mm^3 (15-25 days after transplantation), 250 μl of ODN in different formulations at the dose of 0.625 mg/kg of mouse were administered

by intraperitoneal injection. All work performed with animals was in accordance with and permitted by the Rutgers University, Animal Care and Use committee.

4.3.4 Biodistribution study

Mice with tumor size of ~200-800 mm^3 were i.p injected with Cy5.5-ODN (bcl-2 antisense) in different formulations (0.625 mg/kg). After 24 hrs, mice were killed and tissues were collected and imaged by the IVIS Imaging System (Xenogen Imaging Technologies, Alameda, CA). IVIS imaging allows for live animal imaging, however, as seen in Figure 4.1, the information obtained is semi-quantitative, therefore posing the need to excise organs and quantify whole organ fluorescence. All fluorescence values were adjusted by subtracting autofluorescence from tissues collected from mice treated with PBS. Organs (liver, kidney, heart, spleen, tumor, and lung) were weighed and tumor tissue was immediately homogenized in RLT buffer and stored until mRNA extraction was performed. Fluorescence values were obtained from the same setting throughout the experiment, and values of fluorescence were normalized to mass of kidney, spleen, lung, and liver, and in the case of tumor to the tumor volume (measured by calipers). Blood was collected for quantification of Cy5.5-ODN and to perform cytokine studies.

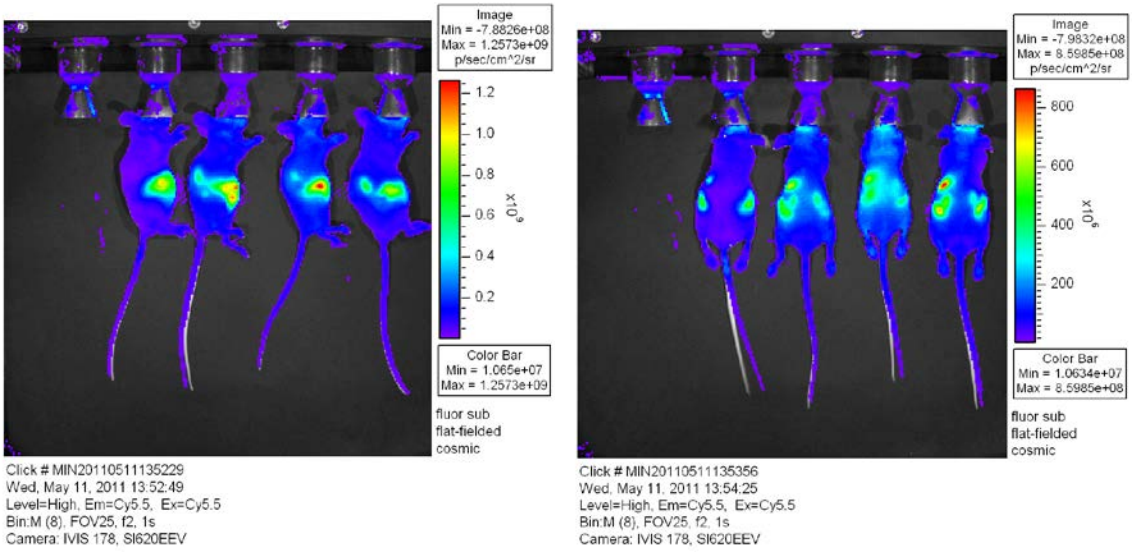

Figure 4.1: Images of live mice upon treatment with DOTAP/ODN complex. Information is semi-quantitative with inability to distinguish fluorescence among organs (kidney, liver, tumor all appear in similar regions) and background signal is high with weak fluorescence intensity from real signal.

4.3.5 Cytokine induction study

Female athymic nude mice were injected with ODN in different formulations at the dose of 0.625 mg ODN/kg. After 24 hours, blood samples were collected and serum was isolated. Tumor necrosis factor, interleukin-6, and interleukin-12 (Biolegend) were measured by enzyme-linked immunosorbent assay according to the manufacturer's protocol. This protocol closely follows that of Li et al. [95].

4.3.6 Gene silencing in a tumor xenograft

Gene silencing from tumors was measured after mice were treated by intratumoral or IP injections (following biodistribution study). Once mice formed tumors of size 200-800 mm3 ODN at 0.625 mg/kg in PPAA-g-1%J70 graft copolymer-delivery system was delivered intratumorally to mice. After 24 hrs post-treatment tumor tissue was excised,

following tissue homogenization and mRNA extraction. Bcl-2 gene expression was normalized to tumors from untreated mice. For IP injection of nanoparticles, after organ imaging, tumor mass was measured and tissue was homogenized. mRNA from cells were extracted using the Qiagen mRNA extraction kit and used to synthesize cDNA (Ambion cDNA synthesis kit) followed by amplification of 18S and Bcl-2 by rt-PCR (using Qiagen Sybr green kit).

4.3.7 Statistics

All statistical analyses were performed by a one-way ANOVA test and results were represented as mean ± standard error (to incorporate differences in the number of mice used per condition). Pair-wise comparisons between the various polymer-containing delivery systems were made using the Tukey HSD post-hoc test; a p-value less than 0.05 indicated significant differences compared with control, as indicated by asterisks on figure plots.

4.4 RESULTS

4.4.1 Biodistribution of nanoparticles 2 hrs- and 24 hrs-post-IP injection

To evaluate the general biodistribution profile of the nanoparticle system in mice, we administered ODN at 0.63 mg/kg in the DOTAP/ODN/PPAA-g-1%J70 and measured Cy5.5 ODN accumulation in excised tissues. The images captured from excised organs are shown in Figure 4.2. Due to unavailability of mice with tumors, the 2 hr time point was conducted using healthy mice. In this figure, we see that at 24 hours post i.p injection, the kidney contains the most fluorescence indicating accumulation of ODN,

followed by the liver, spleen, lung and tumor. At 2 hours post-injection, distribution levels for all these organs are similar.

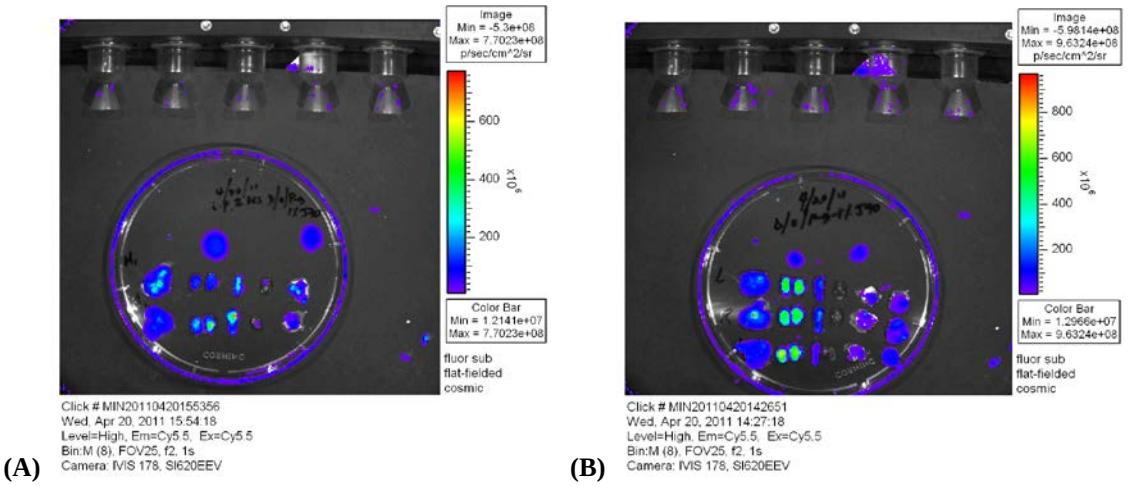

Figure 4.2: Images of excised organs from mice treated with 1% Jeffamine graft copolymer-complex, 2hr- and 24hr- post-treatment (IP injection). Time point 2 hrs indicated in (A) and 24 hrs-post injection (B). Organs on left in (A) in the order- liver, kidney, spleen, heart and lung, and for (B) liver, kidney, spleen, heart, lung and tumor.

4.4.2 Biodistribution of nanoparticles 24 hrs-post-IP injection

The biodistribution profiles of the carriers were evaluated by treating mice with Cy5.5-labeled antisense ODN in the various carrier systems as described in the section 4.3.4 . At the optimum charge ratio of 1, all formulations form complexes with DOTAP/ODN such that ODN is protected with negligible free ODN (data not shown) in solution. This is true for ODN concentrations of 2 μg/ml and lower, which is used for physical and in vitro experiments. A much higher concentration of lipid-polymer complex is required because of the rapid dilution that occurs after injection in vivo and the limitations with the detection limit for Cy5.5 ODN accumulation by IVIS imaging. Under these conditions (ODN concentration of 12.5ug/250ul injection volume),

complexes are formed such that ODN is intact except for the DOTAP/ODN/PPAA complex where ODN precipitates out of solution. Addition of graft copolymer (PPAA-Jeffamine or PPAA-PEO) to DOTAP/ODN stabilizes the complex such that ODN is still intact with the complex, while DOTAP/ODN/PPAA destabilizes the complexes causing ODN to dissociate (data obtained by ODN quenching studies). Hence, for all in vivo experiments the condition with PPAA was eliminated.

We employed Xenogen IVIS imaging system to visualize Cy5.5-ODN distribution in major tissues in the mice 24 hrs after intraperitoneal (IP) injections. This time point was chosen to ensure distribution of Cy5.5 ODN throughout the animal and accumulation in tissues. Although these particles are not targeted, the goal of the in vivo biodistribution studies was to determine whether the lipid-polymer nanoparticles would distribute to xenograft tumors and to assess differences in accumulation of Cy5.5 ODN among nanoparticle formulations incorporating the various polymers of interest. For all conditions, the accumulation of ODN was maximum in the kidney (Fig. 4.3). Accumulation in the spleen was observed for all graft copolymers except DOTAP/ODN, while accumulation in the liver was consistent for all conditions.

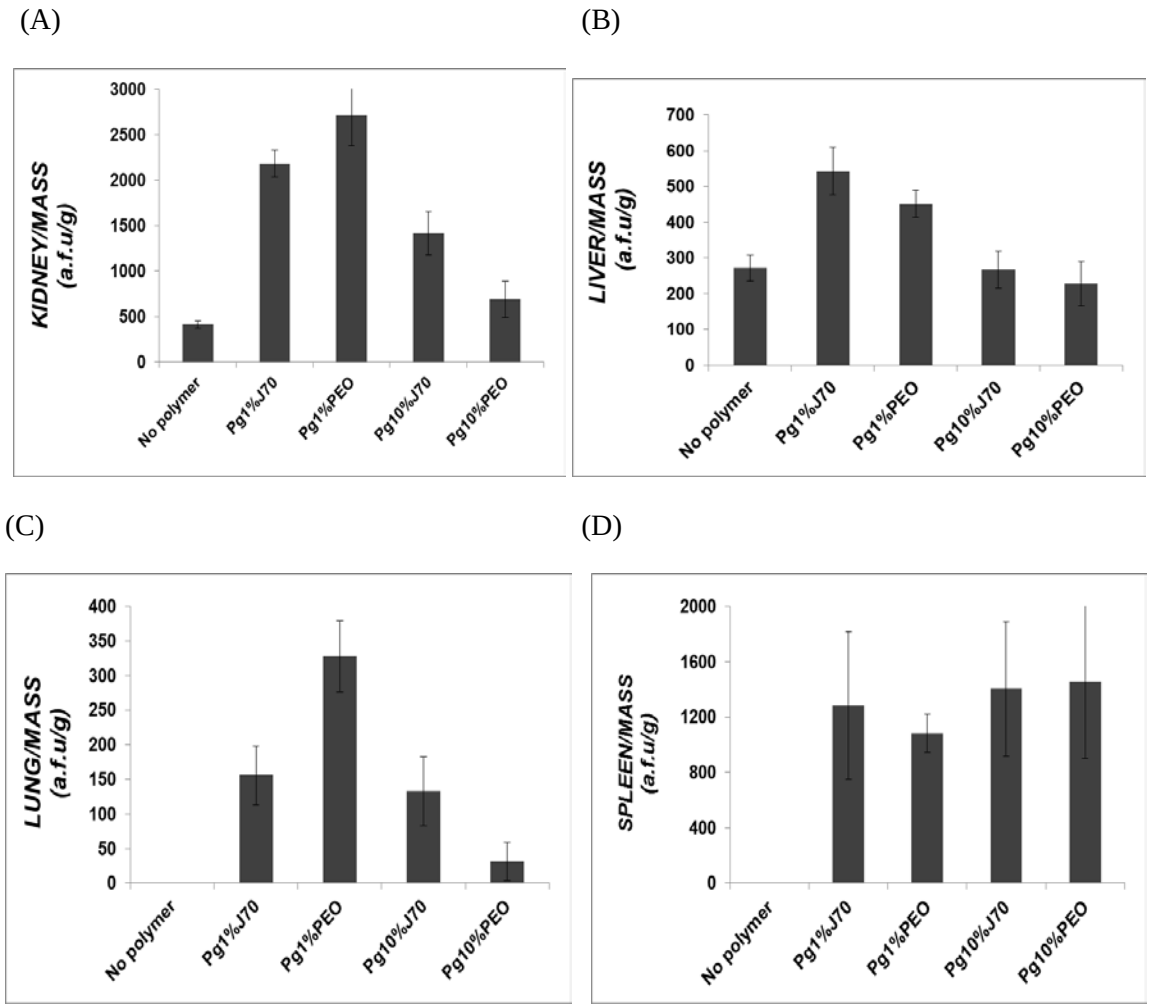

Figure 4.3: Accumulation of Cy5.5-labeled ODN in various animal organs 24 hrs post-treatment of nu/nu athymic mice with nanoparticles by i.p form of injection. All animal were treated with ODN at 0.625 mg/kg mouse. Animal organs were excised and imaged using IVIS imaging system. Fluorescence in kidney (A), liver (B), lung (C) and spleen (D) were normalized to mass (g), and tumor normalized to volume (cm3) Autofluorescence signal from organs was subtracted from fluorescence measured for the conditions for each respective organ. Note: accumulation in heart was negligible. n= 4-6 mice/condition (data represented as standard error mean)

Further, conditions with higher accumulation of ODN in the kidney, PPAA-g-1%J70 and PPAA-g-1%PEO, also showed higher tumor accumulation (Fig. 4.4). Although the accumulation of ODN in the tumor is low for untargeted particles, the serum-stable nanoparticles developed in this study display a significant degree of accumulation in the tumor as measured by IVIS imaging system. Figure 4.4 depicts a comparison of ODN accumulation in the tumor for all the nanoparticle systems. Here, it can be seen that PPAA-g-1%PEO ('Pg1%PEO') followed by PPAA-g-1%Jeffamine M2070 ('Pg1%J70') demonstrate significantly higher ODN accumulation in the tumor compared to control, DOTAP/ODN ('No polymer').

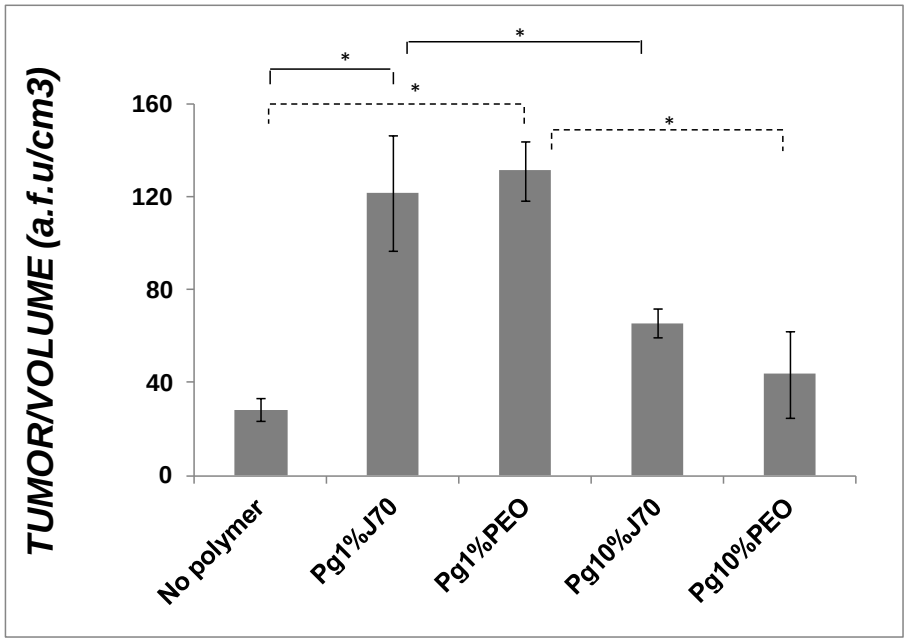

Figure 4.4: Accumulation of Cy5.5-ODN in tumor 24 hrs post-treatment with DOTAP/ODN with 1% and 10% PAO graft copolymers. Tumor fluorescence is normalized to tumor volume (cm3) for each of the conditions. n=4-6 mice/condition (data represented as standard error mean)

4.4.3 Gene silencing and cytokine induction studies

The antisense ODN sequence employed for in vivo studies was dual functional with Cy5.5 tag and antisense sequence specific for bcl-2. This allowed for simultaneous measurement of bcl-2 gene silencing levels in tumor tissues upon treatment with 0.625 mg/kg of ODN. At this dosage, negligible gene silencing effects were observed for any of the graft copolymers when compared to untreated mice (100% bcl-2 gene expression) (data not shown). This indicated that the dosage of antisense ODN that reaches the tumor tissue is not significant to induce a gene silencing effect. As a proof of concept experiment, mice were treated with the DOTAP/ODN/PPAA-g-1%Jeffamine M2070 by intratumoral injection using the same dose as the biodistribution study (0.625mg/kg mouse), and levels of bcl-2 gene silencing as determined by rt-PCR were found to be 47.3±12.4 (with 100% bcl-2 gene expressed represented as control, untreated mice with tumors, n=4 mice)

The immunotoxic effects of the graft copolymers were evaluated by performing ELISA to determine cytokine levels, specifically that of IL-12, TNF-α and IL-6. These cytokines were determined to be important players in stimulating an inflammatory response [95]. It was found that for all the nanoparticles, negligible inflammatory response at the dosage of 0.625 mg ODN/kg mouse was observed, with values than or equal to 7.5 pg/ml for TNF-α and IL-6, and less than or equal to 15 pg/ml for IL-12.

4.5 DISCUSSION

The applications of antisense oligonucleotide drugs are hindered by their negative charge, low stability and rapid blood clearance [96]. The success of antisense or any form of nucleic acid therapy is highly dependent on the development of efficient and non-toxic carriers that will selectively and efficiently deliver cargo to the diseased site, transverse the ECM and other tissue barriers to reach the target cells, and finally gain entry into the interior of cells and exert a therapeutic effect [97, 98]. The design of the carrier and its properties, specifically size, particle surface charge and presence of protective polymer coating, play a crucial role in determining the fate of the antisense once in vivo in blood circulation. Therefore, the success of nanoparticle-based tumor therapy is dependent on circulation time in blood, avoidance of reticuloendothelial system (RES) i.e. the liver & spleen, and renal elimination. The approach in this work has been to incorporate poly (alkylene oxide) (PAO) into the DOTAP liposome/polymer/antisense ODN delivery system, of which poly(ethylene glycol) (PEG) has been most commonly applied. Although, there exist other substitutes of PEG such as poloxamer, polyvinyl alcohol [99], and poly(amino acid)s [100], PEG remains the most widely accepted and characterized approach. For improvement in the biodistribution of liposomes, PEG-lipids such as PEG-DSPE, has been used. The work here has created conjugates of poly (alkylene oxide) (PAO) and pH-sensitive membrane sensitive polymers that are incorporated electrostatically with positively-charged liposomes for the purpose of improving biodistribution profile in vivo by reducing particle surface charge closer to neutrality, as well as enhanced intracellular antisense delivery. The biodistribution studies help to 1) validate in vitro results, 2) determine the optimum grafting of PAO onto PPAA for

liposomal delivery of AONs to the tumor, and 3) understand the influence of carrier characteristics (size, charge, differences in ethylene oxide (EO)/propylene oxide (PO)) chemistries of PEO and Jeffamine, respectively) on RES and kidney clearance of particles, thereby guiding the design of efficient antisense delivery systems for longer blood circulation and desired tumor accumulation.

The biodistribution studies tracked the accumulation of Cy5.5-tagged antisense oligonucleotide to various organs in the mouse, kidney, liver, spleen, lung, heart, and most importantly, the tumor. These particles are not targeted; hence accumulation in the tumor is a result of the enhanced permeation and retention (EPR) effect, a passive form of targeting, which contributes to the movement of long-circulating nanoparticles from the bloodstream and into the tumor interstitium via the leaky vasculature of tumors. The properties of particle size, charge, and presence of alkylene oxide protective group play a role in the distribution of the particles to these various organs. The control carrier, DOTAP/ODN, of particle size of ~400 nm and absence of any protective groups, shows no fluorescent ODN accumulation in the tumor, with majority in the liver and spleen, proving to be taken up by the RES (Fig. 4.3). In comparison, 1 mol% grafting of PEO or Jeffamine M-2070 (ethylene oxide/propylene oxide=3/1), shows significantly higher accumulation in the tumor compared to no polymer and 10 mol% grafting of PEO/Jeffamine (Fig. 4.4). A majority of accumulation of Cy5.5-ODN in the 1 mol% graft copolymer treatments was in the kidney, followed by the spleen and liver, and to a small degree in the lungs. While in comparison, DOTAP/ODN without polymer, showed significantly lower accumulation in the kidney and overall lower whole body fluorescence. We reason that after 24 hours in circulation the more stable grafts of 1

mol% eventually degrade, releasing free Cy5.5-ODN of low molecular weight, which then accumulates in the kidney by the small size/MW cutoff. In the case of the other carriers, this process occurs at a much earlier time point, hence by 24 hours most of the degraded Cy5.5-ODN has already been eliminated.

The effects of chemistry (PEO vs. Jeffamine) chemistries and extent of grafting are revealed in the biodistribution study. At the in vivo level, there seems to be no significant difference between the PEO and Jeffamine (EO/PO=3/1) chemistry, with the 1 mol% grafts of PEO/Jeffamine and 10 mol% grafts of PEO/Jeffamine showing similar ODN accumulation in the tumor and all the other organs. The degree of poly (alkylene oxide) (PAO) seemed to play a role in the biodistribution. While the 1 mol% grafting of PEO or Jeffamine onto PPAA enhanced Cy5.5-ODN delivery, the 10 mol% grafting showed a similar profile to that of unprotected DOTAP/ODN control carrier system with low tumor accumulation and high kidney and liver accumulation. These results indicate that there exists a window of effective grafting densities, after which higher degree of hydrophilicity causes steric hindrance. The 10 mol% grafted polymer shows smaller size nanoparticles of 160 nm compared to 1mol% grafts with 300 nm, however these carrier systems demonstrate lower serum-stability compared to the 1 mol% grafts (as determined by measurement of intact ODN upon incubation with serum). Research groups have found that the architecture of PEG (mushroom vs. brush), PEG molecular weight, and surface chain density play a role in the thickness of the layer around the nanoparticle, which causes improvements in stealth characteristics [21]. Most studies indicate a minimum PEG density, after which an increase in PEGylation provides no additional benefit. Here, we see an optimum where any higher grafting hinders delivery. This

implies that systematic modification of nanoparticles with various degrees of PEG grafting are required to design stable nanoparticles. These results reinforce that the hydrophilic lipophilic balance of the nanoparticle indeed plays a role in dictating in vivo blood circulation and tissue distribution. This knowledge can be exploited to achieve drug accumulation in organs.

CHAPTER 5: DISSERTATION CONCLUSIONS AND FUTURE DIRECTIONS

5.1 Dissertation Summary

In this dissertation, the design and development of a self-assembled nanoparticle for efficient antisense DNA therapeutic delivery is described. The design identifies and targets two key barriers, extracellular serum nuclease degradation and intracellular endosome/lysosome degradation, to create a multi-functional delivery system. The parameters used to guide the design of antisense drug carriers include polymer molecular weight, polymer chemistry, length and density of hydrophilic grafting groups, and overall nanoparticle size and surface charge, are. The central theme of this thesis is to evaluate the effect of hydrophilicity (quantified in terms of a hydrophilic factor 'HF') of polymeric carriers on the efficiency of antisense delivery. The HF of a carrier is hypothesized to be important in 1) dictating the stability of the nanoparticle in the presence of plasma and albumin proteins, which directly influences the biodistribution of nanoparticles, and 2) altering associations of the carrier with cell membranes for entry, and with endosomes to evade intracellular degradation, all of which contribute to the final antisense delivery and gene silencing effect. To study these interactions in a systematic way, a panel of graft copolymers with varying HF was synthesized to study the influence of polymer chemistry on each of the steps involved in the gene delivery process from formulation to tumor delivery in vivo.

For the effect of hydrophilicity on membrane penetration, our observations are consistent with previous literature. That is, increasing hydrophilicity progressively decreases the degree of membrane penetration at pH 7 and pH 5, that of the cytoplasm and endosome, respectively. Therefore, in the presence of non-serum conditions the

parent PPAA polymer system, which is the most hydrophobic (HF of 0), is most efficient in terms of achieving oligonucleotide delivery and gene silencing effects. For the effect of HF on ODN integrity in the presence of serum, an optimum HF exits after which increasing hydrophilicity causes reduced stability of ODN in serum. Finally, we establish a correlation between HF and gene silencing effect, with an optimum HF that yields maximum gene silencing after which increasing HF progressively decreases gene silencing effect. The balance between serum-stability, membrane penetration, and pH-sensitive lysis determines the final antisense delivery, thus bringing to light the need to assess the behavior of carrier modification at all levels in the gene delivery process.

From a therapeutic standpoint, it is critical to evaluate the carrier in an in vivo setting where blood components, RES (reticuloendothelial system) macrophages of the liver, spleen, lymph nodes and bone marrow, EPR effect of leaky tumor vasculature, and ECM environment all play a role in determining the plasma half-life and accumulation of carrier in various organs. Here, parameters of the carrier such as size, particle surface charge, PEG chain length and density, all contribute to determining the fate of the carrier with therapeutic cargo. The delivery of naked nucleic acid leads to an almost instantaneous degradation in the bloodstream or accumulation in kidney by size cutoff of ~10 nm, resulting in renal elimination and urinary excretion. The delivery of nucleic acid using an unprotected carrier (DOTAP/ODN) of size 400 nm and positive zeta potential results in negligible accumulation in the tumor, with majority in the liver and kidney after 24 hours by i.p injection of particles. Surprisingly the 10 mol% hydrophilic grafting, which forms smaller-sized particle of 150 nm, results in poor tumor accumulation, with majority in the kidney and liver. The most efficient delivery system as determined by in

vitro evaluation to be the 1 mol% hydrophilic grafted polymer, which produces neutral particles of ~300 nm size, results in significantly higher tumor accumulation, as well as kidney and liver, compared to the ungrafted and 10 mol% grafted systems. The biodistribution results suggest that the poly (alkylene oxide) graft copolymers remain in blood circulation long enough to accumulate in the tumor by the passive targeting mechanism of EPR. However, most of the ODN that is released in circulation or gets directed from the tumor reaches the kidney, as seen with fluorescent ODN levels still high at 24 hours post-IP injection. For the carrier without graft copolymer, the majority of overall fluorescence from antisense ODN is seen in the liver and spleen as a result of macrophages in these organs that recognize nanoparticles to be foreign, while the remaining ODN is directed to the kidney for clearance. This suggests that the carriers with shorter half-lives are either degraded in the bloodstream, liver or spleen or are cleared renally well before than 24 hour time point. The comparison of no hydrophilic grafting, 1 mol% grafting and 10 mol% grafting in terms of biodistribution of the antisense drug, shows that an appropriate degree of hydrophilic grafting onto a carrier is necessary in yielding tumor accumulation of particles and overall longer circulation of particles in the bloodstream. In order to achieve a therapeutic effect, multiple doses of antisense with chemotherapeutic drug are necessary. A particle with active targeting groups will also increase accumulation of the antisense in the tumor. These are improvements in the system that can be incorporated to increase efficiency of antisense delivery and final therapeutic effect.

5.2 Future Directions

A major improvement in the carrier design is to synthesize particles with 1 mol% hydrophilic grafting, which was determined to be the most effective, however with smaller sizes of ~ 150-200 nm. A potential way to achieve this could be to synthesize DOTAP liposomes from DOTAP lipid and monitoring the size of the liposomes that form and more importantly the distribution of sizes. Another option could involve increasing the DOTAP/ODN charge ratio and optimizing the final charge ratio with polymers at this new condition. By reducing particle size a greater percentage of particles can be directed away from the RES organs and towards the tumor, compared to 300 nm sized particles (Liu, Huang 1992). Other improvements include formation of a nanoparticle that isn't purely based on electrostatic interaction as these interactions are more likely to fall apart in an in vivo system. The antisense ODN can be encapsulated in the DOTAP liposomes during the synthesis of liposomes from lipid, while the graft copolymers can electrostatically interact with the DOTAP/ODN nanoparticle. The system is more controlled and loading of ODN can also be increased. The creation of a more serum-stable system has yielded the graft copolymer conjugate of PPAA and PEO/Jeffamine, and this dual-functional conjugate can be utilized with other carrier systems without being restricted to liposomes. Further, in our recent work with A2780 ovarian cancer cells, we do not notice an added benefit with the Jeffamine vs. PEO; in other words, the presence of propylene oxide groups did not show an enhancement over ethylene oxide groups. However, from our early work we have seen that molecular weight of the parent polymer, PPAA, dictates the overall formation of nanoparticle with DOTAP/ODN and overall hydrophilicity/ hydrophobicity in which case the Jeffamine chemistry plays a role.

More extensive work with varying PPAA molecular weights for grafting needs to be conducted in order to determine this as we have seen differences between 27 and 200k. Further, in our early work we saw dramatic increases by the addition of Jeffamine grafted PPAA compared to PEO, and this may result from free Jeffamine grafted polymer in the formulation that stabilizes the system, but which also may bind with serum proteins indirectly shielding the carrier prior to cell entry. The mechanism of graft copolymer interaction with DOTAP/ODN in the presence of serum environment needs to be explored in greater detail by examining different cell types with varying rates of clathrin and caveolae-mediated endocytosis routes of entry. Another aspect of this delivery system is for the application of chemotherapeutic drug delivery. In this work, the co-delivery of drugs and antisense ODN using the DOTAP/polymer carrier system has been found to yield synergistic toxic effects with 80% toxicity at a fixed concentration of doxorubicin, compared to 65% toxicity with combined delivery of doxorubicin and bcl-2 antisense. This work can be explored in vivo where the key advantage would be lower number of injections and targeting both chemotherapeutic and antisense drugs to the diseased cells.

REFERENCES

1. Hannun, Y.A., *Apoptosis and the dilemma of cancer chemotherapy.* Blood, 1997. **89**(6): p. 1845-53.
2. Nguyen, H.K., et al., *Evaluation of polyether-polyethyleneimine graft copolymers as gene transfer agents.* Gene Ther, 2000. **7**(2): p. 126-38.
3. Gleave, M.E. and B.P. Monia, *Antisense therapy for cancer.* Nat Rev Cancer, 2005. **5**(6): p. 468-79.
4. Monia, B.P., et al., *Evaluation of 2'-modified oligonucleotides containing 2'-deoxy gaps as antisense inhibitors of gene expression.* J Biol Chem, 1993. **268**(19): p. 14514-22.
5. Potera, C., *Antisense-down, but not out.* Nature Biotechnology, 2007. **25**(5): p. 497-499.
6. Klasa, R.J., et al., *Oblimersen Bcl-2 antisense: facilitating apoptosis in anticancer treatment.* Antisense Nucleic Acid Drug Dev, 2002. **12**(3): p. 193-213.
7. Kang, M.H. and C.P. Reynolds, *Bcl-2 inhibitors: targeting mitochondrial apoptotic pathways in cancer therapy.* Clin Cancer Res, 2009. **15**(4): p. 1126-32.
8. Kim, R., et al., *Antisense and nonantisense effects of antisense Bcl-2 on multiple roles of Bcl-2 as a chemosensitizer in cancer therapy.* Cancer Gene Ther, 2007. **14**(1): p. 1-11.
9. Beh, C.W., et al., *Efficient delivery of Bcl-2-targeted siRNA using cationic polymer nanoparticles: downregulating mRNA expression level and sensitizing cancer cells to anticancer drug.* Biomacromolecules, 2009. **10**(1): p. 41-8.
10. Moulder, S.L., et al., *Phase I/II study of G3139 (Bcl-2 antisense oligonucleotide) in combination with doxorubicin and docetaxel in breast cancer.* Clin Cancer Res, 2008. **14**(23): p. 7909-16.
11. Piro, L.D., *Apoptosis, Bcl-2 antisense, and cancer therapy.* Oncology (Williston Park), 2004. **18**(13 Suppl 10): p. 5-10.
12. Kuo, M.T., *Redox regulation of multidrug resistance in cancer chemotherapy: molecular mechanisms and therapeutic opportunities.* Antioxid Redox Signal, 2009. **11**(1): p. 99-133.
13. Linn, S.C., et al., *Expression of drug resistance proteins in breast cancer, in relation to chemotherapy.* Int J Cancer, 1997. **71**(5): p. 787-95.
14. Kuo, M.T., *Roles of multidrug resistance genes in breast cancer chemoresistance.* Adv Exp Med Biol, 2007. **608**: p. 23-30.
15. McMahon, B.M., et al., *Pharmacokinetics and tissue distribution of a peptide nucleic acid after intravenous administration.* Antisense Nucleic Acid Drug Dev, 2002. **12**(2): p. 65-70.
16. Frank, M.M. and L.F. Fries, *The role of complement in inflammation and phagocytosis.* Immunol Today, 1991. **12**(9): p. 322-6.
17. Johnson, R., *The complement system*. Biomaterials Science: An Introduction to Materials in Medicine, ed. A.S.H. B.D. Ratner, F.J. Schoen, J.E. Lemons2004: Elsevier Academic Press, Amsterdam. 318–328.
18. Huang, L., Li S-D, *Pharmacokinetics and Biodistribution of Nanoparticles.* Molecular pharmaceutics, 2008. **5**(4): p. 496-504.

19. Carrstensen, H., R.H. Muller, and B.W. Muller, *Particle size, surface hydrophobicity and interaction with serum of parenteral fat emulsions and model drug carriers as parameters related to RES uptake.* Clin Nutr, 1992. **11**(5): p. 289-97.
20. Gref, R., et al., *Biodegradable long-circulating polymeric nanospheres.* Science, 1994. **263**(5153): p. 1600-3.
21. Owens, D.E., 3rd and N.A. Peppas, *Opsonization, biodistribution, and pharmacokinetics of polymeric nanoparticles.* Int J Pharm, 2006. **307**(1): p. 93-102.
22. White, P.J., et al., *Overcoming biological barriers to in vivo efficacy of antisense oligonucleotides.* Expert Rev Mol Med, 2009. **11**: p. e10.
23. Sledge, G.W., Jr. and K.D. Miller, *Exploiting the hallmarks of cancer: the future conquest of breast cancer.* Eur J Cancer, 2003. **39**(12): p. 1668-75.
24. Hobbs, S.K., et al., *Regulation of transport pathways in tumor vessels: role of tumor type and microenvironment.* Proc Natl Acad Sci U S A, 1998. **95**(8): p. 4607-12.
25. Yuan, F., et al., *Vascular permeability in a human tumor xenograft: molecular size dependence and cutoff size.* Cancer Res, 1995. **55**(17): p. 3752-6.
26. Couvreur, P. and C. Vauthier, *Nanotechnology: intelligent design to treat complex disease.* Pharm Res, 2006. **23**(7): p. 1417-50.
27. Torchilin, V.P., *Recent advances with liposomes as pharmaceutical carriers.* Nat Rev Drug Discov, 2005. **4**(2): p. 145-60.
28. Jain, R.K. and T. Stylianopoulos, *Delivering nanomedicine to solid tumors.* Nat Rev Clin Oncol. **7**(11): p. 653-64.
29. Roth, C.M. and S. Sundaram, *Engineering synthetic vectors for improved DNA delivery: insights from intracellular pathways.* Annu Rev Biomed Eng, 2004. **6**: p. 397-426.
30. Akhtar, S., et al., *The delivery of antisense therapeutics.* Adv Drug Deliv Rev, 2000. **44**(1): p. 3-21.
31. Wong, S.Y., N. Sood, and D. Putnam, *Combinatorial evaluation of cations, pH-sensitive and hydrophobic moieties for polymeric vector design.* Mol Ther, 2009. **17**(3): p. 480-90.
32. Lungwitz, U., et al., *Polyethylenimine-based non-viral gene delivery systems.* Eur J Pharm Biopharm, 2005. **60**(2): p. 247-66.
33. Neu, M., D. Fischer, and T. Kissel, *Recent advances in rational gene transfer vector design based on poly(ethylene imine) and its derivatives.* J Gene Med, 2005. **7**(8): p. 992-1009.
34. Tiera, M.J., et al., *Polycation-based gene therapy: current knowledge and new perspectives.* Curr Gene Ther. **11**(4): p. 288-306.
35. Kim, J., et al., *Enhancement of polyethylene glycol (PEG)-modified cationic liposome-mediated gene deliveries: effects on serum stability and transfection efficiency.* Journal of Pharmacy and Pharmacology, 2003. **55**(4): p. 453.
36. Kyriakides, T.R., et al., *pH-sensitive polymers that enhance intracellular drug delivery in vivo.* J Control Release, 2002. **78**(1-3): p. 295-303.

37. Kabanov, A.V., et al., *Polymer genomics: shifting the gene and drug delivery paradigms.* J Control Release, 2005. **101**(1-3): p. 259-71.
38. Abraham, S.A., et al., *The liposomal formulation of doxorubicin.* Methods Enzymol, 2005. **391**: p. 71-97.
39. Kalra, A.V. and R.B. Campbell, *Development of 5-FU and doxorubicin-loaded cationic liposomes against human pancreatic cancer: Implications for tumor vascular targeting.* Pharm Res, 2006. **23**(12): p. 2809-17.
40. Schmitt-Sody, M., et al., *Neovascular targeting therapy: paclitaxel encapsulated in cationic liposomes improves antitumoral efficacy.* Clin Cancer Res, 2003. **9**(6): p. 2335-41.
41. Campbell, R.B., et al., *Fighting cancer: from the bench to bedside using second generation cationic liposomal therapeutics.* J Pharm Sci, 2009. **98**(2): p. 411-29.
42. Kim, J.K., et al., *Enhancement of polyethylene glycol (PEG)-modified cationic liposome-mediated gene deliveries: effects on serum stability and transfection efficiency.* J Pharm Pharmacol, 2003. **55**(4): p. 453-60.
43. Murthy, N., et al., *Design and synthesis of pH-responsive polymeric carriers that target uptake and enhance the intracellular delivery of oligonucleotides.* J Control Release, 2003. **89**(3): p. 365-74.
44. Davis, M.E., Z.G. Chen, and D.M. Shin, *Nanoparticle therapeutics: an emerging treatment modality for cancer.* Nat Rev Drug Discov, 2008. **7**(9): p. 771-82.
45. Petros, R.A. and J.M. DeSimone, *Strategies in the design of nanoparticles for therapeutic applications.* Nat Rev Drug Discov. **9**(8): p. 615-27.
46. Kabanov, A., J. Zhu, and V. Alakhov, *Pluronic block copolymers for gene delivery.* Adv Genet, 2005. **53**: p. 231-61.
47. Liaw, J., S.F. Chang, and F.C. Hsiao, *In vivo gene delivery into ocular tissues by eye drops of poly(ethylene oxide)-poly(propylene oxide)-poly(efhylene oxide) (PEO-PPO-PEO) polymeric micelles.* Gene Therapy, 2001. **8**(13): p. 999-1004.
48. Kabanov, A.V., et al., *Pluronic((R)) block copolymers: novel functional molecules for gene therapy.* Advanced Drug Delivery Reviews, 2002. **54**(2): p. 223-233.
49. Pitard, B., et al., *Amphiphilic block copolymers promote gene delivery in vivo to pathological skeletal muscles.* Human Gene Therapy, 2005. **16**(11): p. 1318-1324.
50. Alakhov, V.Y., et al., *Altered organ accumulation of oligonucleotides using polyethyleneimine grafted with poly(ethylene oxide) or pluronic as carriers.* Journal of Drug Targeting, 2002. **10**(2): p. 113-121.
51. Chow, T.Y.K., et al., *Polyethyleneimine grafted with pluronic P85 enhances Ku86 antisense delivery and the ionizing radiation treatment efficacy in vivo.* Gene Therapy, 2004. **11**(22): p. 1665-1672.
52. Alexis, F., et al., *Factors affecting the clearance and biodistribution of polymeric nanoparticles.* Mol Pharm, 2008. **5**(4): p. 505-15.
53. Peer, D., et al., *Nanocarriers as an emerging platform for cancer therapy.* Nat Nanotechnol, 2007. **2**(12): p. 751-60.
54. Haley, B. and E. Frenkel, *Nanoparticles for drug delivery in cancer treatment.* Urologic oncology, 2008. **26**(1): p. 57-64.

55. Huang, L. and Y. Liu, *In vivo delivery of RNAi with lipid-based nanoparticles.* Annu Rev Biomed Eng. **13**: p. 507-30.
56. Liu, Z., J. Janzen, and D.E. Brooks, *Adsorption of amphiphilic hyperbranched polyglycerol derivatives onto human red blood cells.* Biomaterials. **31**(12): p. 3364-73.
57. Moreira, J.N., R. Gaspar, and T.M. Allen, *Targeting Stealth liposomes in a murine model of human small cell lung cancer.* Biochim Biophys Acta, 2001. **1515**(2): p. 167-76.
58. Arvizo, R.R., et al., *Modulating pharmacokinetics, tumor uptake and biodistribution by engineered nanoparticles.* PLoS One. **6**(9): p. e24374.
59. Levchenko, T.S., et al., *Liposome clearance in mice: the effect of a separate and combined presence of surface charge and polymer coating.* Int J Pharm, 2002. **240**(1-2): p. 95-102.
60. Zhang, Y. and T.J. Anchordoquy, *The role of lipid charge density in the serum stability of cationic lipid/DNA complexes.* Biochim Biophys Acta, 2004. **1663**(1-2): p. 143-57.
61. Yamamoto, Y., et al., *Long-circulating poly(ethylene glycol)-poly(D,L-lactide) block copolymer micelles with modulated surface charge.* J Control Release, 2001. **77**(1-2): p. 27-38.
62. Wang, B., et al., *Effects of hydrophobic and hydrophilic modifications on gene delivery of amphiphilic chitosan based nanocarriers.* Biomaterials. **32**(20): p. 4630-8.
63. Liu, Z., Zhang, Z., Zhou, C., Jiao, Y, *Hydrophobic modifications of cationic polymers for gene delivery.* Progress in Polymer Science, 2010. **35**(9).
64. Alshamsan, A., et al., *Formulation and delivery of siRNA by oleic acid and stearic acid modified polyethylenimine.* Mol Pharm, 2009. **6**(1): p. 121-33.
65. Philipp, A., et al., *Hydrophobically modified oligoethylenimines as highly efficient transfection agents for siRNA delivery.* Bioconjug Chem, 2009. **20**(11): p. 2055-61.
66. Creusat, G. and G. Zuber, *Self-assembling polyethylenimine derivatives mediate efficient siRNA delivery in mammalian cells.* Chembiochem, 2008. **9**(17): p. 2787-9.
67. Bromberg, L., et al., *Guanidinylated polyethyleneimine-polyoxypropylene-polyoxyethylene conjugates as gene transfection agents.* Bioconjug Chem, 2009. **20**(5): p. 1044-53.
68. Bromberg, L., et al., *Polycationic block copolymers of poly(ethylene oxide) and poly(propylene oxide) for cell transfection.* Bioconjug Chem, 2005. **16**(3): p. 626-33.
69. Gebhart, C.L., et al., *Design and formulation of polyplexes based on pluronic-polyethyleneimine conjugates for gene transfer.* Bioconjug Chem, 2002. **13**(5): p. 937-44.
70. Takahashi, T., et al., *Alkyl chain moieties of polyamidoamine dendron-bearing lipids influence their function as a nonviral gene vector.* Bioconjug Chem, 2007. **18**(4): p. 1349-54.

71. Gref, R., et al., *'Stealth' corona-core nanoparticles surface modified by polyethylene glycol (PEG): influences of the corona (PEG chain length and surface density) and of the core composition on phagocytic uptake and plasma protein adsorption.* Colloids Surf B Biointerfaces, 2000. **18**(3-4): p. 301-313.
72. Nagayama, S., et al., *Time-dependent changes in opsonin amount associated on nanoparticles alter their hepatic uptake characteristics.* Int J Pharm, 2007. **342**(1-2): p. 215-21.
73. Fang, C., et al., *In vivo tumor targeting of tumor necrosis factor-alpha-loaded stealth nanoparticles: effect of MePEG molecular weight and particle size.* Eur J Pharm Sci, 2006. **27**(1): p. 27-36.
74. Lee, L.K., et al., *Poly(propylacrylic acid) enhances cationic lipid-mediated delivery of antisense oligonucleotides.* Biomacromolecules, 2006. **7**(5): p. 1502-8.
75. Lee, M. and S.W. Kim, *Polyethylene glycol-conjugated copolymers for plasmid DNA delivery.* Pharm Res, 2005. **22**(1): p. 1-10.
76. Roux, E., et al., *Serum-stable and long-circulating, PEGylated, pH-sensitive liposomes.* J Control Release, 2004. **94**(2-3): p. 447-51.
77. Murthy, N., et al., *The design and synthesis of polymers for eukaryotic membrane disruption.* J Control Release, 1999. **61**(1-2): p. 137-43.
78. Cheung, C.Y., et al., *A pH-sensitive polymer that enhances cationic lipid-mediated gene transfer.* Bioconjug Chem, 2001. **12**(6): p. 906-10.
79. Sundaram, S., L.K. Lee, and C.M. Roth, *Interplay of polyethyleneimine molecular weight and oligonucleotide backbone chemistry in the dynamics of antisense activity.* Nucleic Acids Res, 2007. **35**(13): p. 4396-408.
80. Moore, J., Stupp, SI, *Cleavage of Aldehyde Hydrazonium Iodides Under Mild Conditions. A Convenient Route to Chiral Nitriles of High Enantiomeric Purity.* Journal of Organic Chemistry, 1990. **55**: p. 3374.
81. Hourdet D, L.A.F., Audebert R, *Synthesis of thermoassociative copolymers.* Polymer, 1997. **38**(10): p. 2535-2547.
82. Kusonwiriyawong, C., et al., *Evaluation of pH-dependent membrane-disruptive properties of poly(acrylic acid) derived polymers.* Eur J Pharm Biopharm, 2003. **56**(2): p. 237-46.
83. Lucas, B., et al., *Towards a better understanding of the dissociation behavior of liposome-oligonucleotide complexes in the cytosol of cells.* J Control Release, 2005. **103**(2): p. 435-50.
84. Duncan, R. and L. Izzo, *Dendrimer biocompatibility and toxicity.* Adv Drug Deliv Rev, 2005. **57**(15): p. 2215-37.
85. Cho, Y.W., J.D. Kim, and K. Park, *Polycation gene delivery systems: escape from endosomes to cytosol.* J Pharm Pharmacol, 2003. **55**(6): p. 721-34.
86. Verma, A. and F. Stellacci, *Effect of surface properties on nanoparticle-cell interactions.* Small. **6**(1): p. 12-21.
87. Moghimi, S.M., A.C. Hunter, and J.C. Murray, *Long-circulating and target-specific nanoparticles: theory to practice.* Pharmacol Rev, 2001. **53**(2): p. 283-318.

88. Rejman, J., et al., *Size-dependent internalization of particles via the pathways of clathrin- and caveolae-mediated endocytosis.* Biochem J, 2004. **377**(Pt 1): p. 159-69.
89. Hamidi, M., A. Azadi, and P. Rafiei, *Pharmacokinetic consequences of pegylation.* Drug Deliv, 2006. **13**(6): p. 399-409.
90. Peddada, L.Y., et al., *Novel graft copolymers enhance in vitro delivery of antisense oligonucleotides in the presence of serum.* J Control Release, 2009. **140**(2): p. 134-40.
91. John Wiley and Sons, *Colloids and interfaces with surfactants and polymers: an introduction* J.W. Goodwin, Editor 2004: England.
92. Simoes, S., et al., *On the formulation of pH-sensitive liposomes with long circulation times.* Adv Drug Deliv Rev, 2004. **56**(7): p. 947-65.
93. Choi, H.S., et al., *Design considerations for tumour-targeted nanoparticles.* Nat Nanotechnol. **5**(1): p. 42-7.
94. Pakunlu, R.I., et al., *In vitro and in vivo intracellular liposomal delivery of antisense oligonucleotides and anticancer drug.* J Control Release, 2006. **114**(2): p. 153-62.
95. Li, S.D., et al., *Tumor-targeted delivery of siRNA by self-assembled nanoparticles.* Molecular therapy : the journal of the American Society of Gene Therapy, 2008. **16**(1): p. 163-9.
96. Juliano, R., et al., *Biological barriers to therapy with antisense and siRNA oligonucleotides.* Mol Pharm, 2009. **6**(3): p. 686-95.
97. Huang, L. and M. Nishikawa, *Nonviral vectors in the new millennium: Delivery barriers in gene transfer.* Human Gene Therapy, 2001. **12**(8): p. 861-870.
98. Pack, D.W., et al., *Design and development of polymers for gene delivery.* Nature Reviews Drug Discovery, 2005. **4**(7): p. 581-593.
99. Takeuchi, H., et al., *Polymer coating of liposomes with a modified polyvinyl alcohol and their systemic circulation and RES uptake in rats.* Journal of controlled release : official journal of the Controlled Release Society, 2000. **68**(2): p. 195-205.
100. Metselaar, J.M., et al., *A novel family of L-amino acid-based biodegradable polymer-lipid conjugates for the development of long-circulating liposomes with effective drug-targeting capacity.* Bioconjugate Chemistry, 2003. **14**(6): p. 1156-64.

CURRICULUM VITAE
LAVANYA Y. PEDDADA

Education

January 2012 Rutgers, State University of New Jersey, New Brunswick, NJ
Ph.D. Biomedical Engineering
May 2005 University of Virginia, Charlottesville, Virginia
B.S. Chemical Engineering

Principal Occupation

Rutgers, The State University of New Jersey, Piscataway, NJ
Graduate Researcher to Dr. Charles Roth (PhD Advisor) 2006-2011

Institute of Bioengineering and Nanotechnology, Singapore
Summer intern, Supervisor: Dr. Yi-Yan Yang July– Aug 2008

Rutgers, The State University of New Jersey, Piscataway, NJ
Teaching Assistant 2008-2009

Bristol-Myers Squibb, Oncology Department, Lawrenceville, NJ
Research Intern (Supervisor: Dr. Maria Jure-Kunkel) June-Aug 2004

Peer-reviewed publications & Patents

1. Graft polymers for enhanced intracellular delivery of antisense molecules (United States Patent Application 12/744824) (Contributed to data generation)

2. **Peddada LY**, Harris NK, Devore DI, Roth CM "Novel graft copolymers enhance in vitro delivery of antisense oligonucleotides in the presence of serum". J Control Release 2009 Dec 3; 140 (2): 134-40 (First-author)

3. Mishra S, **Peddada LY**, Devore DI, Roth CM "Poly (alkylene oxide) copolymers for nucleic acid delivery", Accounts of Chemical Research (Submitted Sept. 2011) (Co-first author)

4. **Peddada LY**, et al "Antisense delivery to tumor using poly (alkylene oxide) conjugates in a self-assembled liposomal nanoparticle" (Manuscript for submission in Jan 2012)